
Evaluation of new data sources for improving the estimation of background concentrations in Norway

Philipp Schneider and Andrzej Obracaj



Scientific report

Contents

1	Introduction and Background	9
2	Data	15
2.1	Station data	15
2.2	Satellite NO ₂ data	16
2.3	ETC/ACM data	18
2.4	CHIMERE Model Data	19
3	Methodology	21
3.1	Satellite Retrieval Methodology	21
3.2	Geostatistical framework	22
4	Results and Discussion	25
4.1	Using satellite data	25
4.1.1	Choosing a suitable satellite product	25
4.1.2	Kriging NO ₂ in Norway using Airbase and OMI satellite data . .	31
4.2	Using model output	38
4.2.1	NO ₂	39
4.2.2	O ₃	39
4.2.3	PM ₁₀	41
4.2.4	PM _{2.5}	43
4.2.5	Evaluation for estimation of background concentrations in Nor- way	47
4.3	Web mapping system	48
5	Conclusions	53

List of Figures

1	Matrix visualization of NO ₂ at station <i>NO0075A Barnehaugen</i>	11
2	Comparison of information content	12
3	Maps of 2007 (NO ₂) and 2008 annual means of NO ₂ , O ₃ , PM ₁₀ , and PM _{2.5} as they were computed in the 2011 study	13
4	Map showing the 2009 average NO ₂ concentration measured at all Airbase background stations. (from Schneider et al. (2011))	15
5	Map of background stations used for mapping and temporal decomposition	17
6	Example of an empirical semivariogram $\hat{\gamma}(h)$ and its model	23
7	Schematic of the general methodology	24
8	Annual mean NO ₂ concentration for the year 2009 derived from the OMNO2e daily 0.25° × 0.25° product	26
9	Annual mean NO ₂ concentration for the year 2009 derived from the SCIAMACHY/TEMIS monthly 0.25° × 0.25° product	27
10	Difference image of the mean annual NO ₂ column retrieved from SCIAMACHY and OMI	28
11	The 0.1° × 0.1° resolution OMNO2e product over Europe. Shown here is the 2009 annual mean tropospheric NO ₂ concentration	29
12	Comparison of the 0.25° × 0.25° resolution OMNO2e product (top) with the 0.1 degree resolution OMNO2e product (bottom), shown for the Po valley region in Northern Italy	30
13	Annual average tropospheric NO ₂ column for the year 2009 over Norway. Derived from the 0.1 degree high-resolution OMNO2e product	31
14	Scatterplot of Airbase-derived annual mean 2009 station NO ₂ concentration against the 2009 annual mean tropospheric NO ₂ columns derived from the OMNO2e high-resolution product.	32
15	Empirical and modeled semivariogram of the residuals	33
16	Map showing the residuals from the model fitted between the average 2009 NO ₂ at all Airbase background stations and the mean tropospheric NO ₂ column provided by the high-resolution OMNO2e product.	34
17	Map showing the residuals from the model fitted between the average 2009 NO ₂ at all Airbase background stations in Norway and the mean tropospheric NO ₂ column provided by the high-resolution OMNO2e product	35
18	Map showing the geostatistically interpolated residuals given at the station level in Figure 16	36
19	The average NO ₂ concentration in Norway for 2009	37
20	Annual mean NO ₂ concentration over southern Norway as computed by the CHIMERE chemical transport model.	38
21	Comparison of 2009 hourly time series of NO ₂ from station measurements in southern Norway and the corresponding time series extracted from the CHIMERE output over the same locations.	40
22	Comparison of 2009 hourly time series of NO ₂ from station measurements in southern Norway and the corresponding time series extracted from the CHIMERE output over the same locations, here shown as a two-dimensional histograms (or density plots).	41

23	Comparison of 2009 hourly time series of O ₃ from station measurements in southern Norway and the corresponding time series extracted from the CHIMERE output over the same locations.	42
24	Comparison of 2009 hourly time series of O ₃ from station measurements in southern Norway and the corresponding time series extracted from the CHIMERE output over the same locations, here shown as two-dimensional histograms (or density plots).	43
25	Comparison of 2009 hourly time series of PM ₁₀ from station measurements in southern Norway and the corresponding time series extracted from the CHIMERE output over the same locations.	44
26	Comparison of 2009 hourly time series of PM ₁₀ from station measurements in southern Norway and the corresponding time series extracted from the CHIMERE output over the same locations, here shown as a two-dimensional histograms (or density plots).	45
27	Comparison of 2009 hourly time series of PM _{2.5} from station measurements in southern Norway and the corresponding time series extracted from the CHIMERE output over the same locations.	46
28	Comparison of 2009 hourly time series of PM _{2.5} from station measurements in southern Norway and the corresponding time series extracted from the CHIMERE output over the same locations, here shown as two-dimensional histograms (or density plots).	46
29	Screenshot of the mapping component of the online web mapping application	49
30	As Figure 29, here showing background concentrations of PM ₁₀ in the greater Oslo area	50
31	As Figure 29, here showing background concentrations of O ₃ in the Lillehammer area.	51
32	Example screenshot of downloaded data	52

List of Tables

1	Overview of Norwegian background air quality stations that were used for temporal characterization	16
2	Overview of station type and components measured at each station as well as their respective long-term mean	18
3	Result of simple linear regression between the 2009 hourly time series of NO ₂ from station measurements in southern Norway and the corresponding time series extracted from the CHIMERE output over the same locations.	39
4	Result of simple linear regression between the 2009 hourly time series of O ₃ from station measurements in southern Norway and the corresponding time series extracted from the CHIMERE output over the same locations.	42
5	Result of simple linear regression between the 2009 hourly time series of PM ₁₀ from station measurements in southern Norway and the corresponding time series extracted from the CHIMERE output over the same locations.	44
6	Result of simple linear regression between the 2009 hourly time series of PM _{2.5} from station measurements in southern Norway and the corresponding time series extracted from the CHIMERE output over the same locations.	46

Summary

Based on the experience gained as part of a previous project on developing an “atlas” of background concentrations for NO₂, O₃, PM₁₀, and PM_{2.5} over Norway (Schneider et al., 2011), additional work has been carried out in order to evaluate potential improvements to the existing dataset. Both the previous work and this follow-up project were funded by the Climate and Pollution Agency of Norway (KLIF). Three major objectives were addressed as part of this work:

1. To evaluate the potential of satellite-derived NO₂ data for improving station-based NO₂ mapping in Norway
2. To evaluate the feasibility of using data from a high-resolution atmospheric model for better spatial and temporal characterization of background concentrations
3. To make the results available through an online web mapping system to allow easy access to the data and to provide basic visualization of the results

In order to evaluate the potential of satellite data for mapping air quality, different satellite products providing information on NO₂ were first tested and compared. An experimental high-resolution product acquired by the Ozone Mapping Instrument (OMI) on board of the National Aeronautics and Space Administration's Aura platform was identified as the most suitable product with respect to its similarity to future datasets to be acquired by satellites associated with the Global Monitoring for Environment and Security (GMES) initiative. This product was then used as an auxiliary dataset to guide the spatial interpolation of NO₂ station data. The results indicate that the satellite dataset is useful in providing information on spatial patterns in areas with very low station density such as Norway. Using a simple cross-validation scheme it was shown that a kriging procedure involving OMI-based auxiliary data allowed for mapping NO₂ with a lower overall root mean squared error than when using ordinary kriging on station data alone.

In a second task, the output from a high-resolution run of the chemical transport model CHIMERE was evaluated with respect to its ability to contribute to estimating the background concentrations over Norway. This was accomplished using a comparative analysis of station observations with CHIMERE-derived time series at the same location. Using a linear regression model the correlation between the two datasets was then studied for several stations and atmospheric pollutants. The results indicate that, with exception of O₃, the CHIMERE-derived hourly time series are generally only weakly correlated with the actual station observations, at least with respect to high-frequency temporal variability. This fact, combined with the lack of long time series of high resolution model output, makes the use of this dataset challenging for temporal characterization of the background concentrations. However, the data is still very valuable as an auxiliary dataset for providing spatial information to assist a geostatistical interpolation of station data.

Finally, in the third task of this study, a web-based mapping portal was developed in order to provide flexible access to the data and to basic visualization tools. The web site provides a Geoserver-based environment for exploring the data by freely zooming and panning in a map interface and further offers the possibility for displaying and downloading customized time series for the various pollutants at any point within Norway.

1 Introduction and Background

Knowing the average or typical background concentration of atmospheric pollutants such as O₃, NO₂, PM₁₀, and PM_{2.5} at a given point in space and time is critical for a variety of applications, and in particular for a comprehensive assessment of air quality. For this reason, the Climate and Pollution Agency of Norway (KLIF) contracted the Norwegian Institute for Air Research (NILU) in 2011 to develop a first version of an atlas of background concentrations of various pollutants for Norway and thereby to update the previously used estimates of background concentrations based on the VLUFT tool. The report summarizing the work carried out in 2011 (Schneider et al., 2011) describes in detail the methodology used for this purpose. In addition, it lists several simplifications and error sources of the present methodology and suggests possible solutions. One of the recommendations in this report was to examine other auxiliary datasets such as satellite and model output for their potential to providing additional information to the methodology.

In 2012, additional funding was provided for evaluating additional auxiliary datasets regarding their potential of improving the spatial and temporal characterization of the background concentration estimates. This follow-up project focused on three major objectives:

1. To evaluate the potential of satellite-derived NO₂ data for improving station-based NO₂ mapping in Norway
2. To evaluate the feasibility of using data from a high-resolution atmospheric model for better spatial and temporal characterization of background concentrations
3. To make the results available through an online web mapping system to allow easy access to the data and to provide basic visualization of the results

The work carried out in this project in order to achieve these objectives is to a large extent based on the methodology developed in 2011. Therefore, a brief summary of the existing methodology is provided in the following. More details including a comprehensive description of the used data sets can be found in the previous report provided by Schneider et al. (2011).

The estimation of Norwegian background concentrations for NO₂, O₃, PM₁₀, and PM_{2.5} as carried out in 2011 is based on two main components. The first component consists of maps of the average annual background concentration for recent years that are derived from station observations in conjunction with spatially distributed auxiliary data using geostatistical techniques. However, since most of the pollutants considered here vary significantly with time, maps of annual averages alone are not sufficient. The second component of the methodology is therefore based on a quantitative description of the average long-term temporal behavior of the observations at each station (Schneider et al., 2011).

A combination of the two components was then accomplished within the framework of this project by averaging several years of hourly measurements on an annual as well as on a daily basis. The resulting time series for a typical year and a typical day were further smoothed to ensure that the observations are representative of cyclical temporal patterns and do not just reflect short-term variability. The representative annual and daily time series are subsequently converted from absolute concentrations given in $\mu\text{g m}^{-3}$ to anomalies from the long-term mean at the station given in percent.

This ensures the applicability of the temporal information for neighboring areas with differing mean annual background concentrations.

Due to the often short time series available at each station and the associated small sample size, random noise which is not representative of the overall long-term temporal variability is abundant in the time series and needs to be removed before using the relative anomalies for estimating concentrations at other locations. Such a task can for example be performed by using a moving average filter. However, for practical purposes this smoothing was performed here in the operational application by applying a two-dimensional low-pass filter on an hour-by-hour anomaly matrix for an average year. This results in a simultaneous smoothing of both the annual and daily average time series. An example is shown in Figure 1. It should be noted that the application of the filter was performed while the matrix was augmented by itself on all four sides in order to avoid erroneous edge effects caused by the filter.

The smoothed relative anomalies can then be applied to neighboring locations with different absolute annual mean concentrations, and as such the average concentration can be estimated for a certain location given a certain day of the year and a time of day.

Figure 2 shows a comparison of the information content provided by the updated background concentration as opposed to the previously used 1993 VLUFT data set. Compared to the previously used VLUFT dataset, the method presented here has clear advantages in that it provides a significantly higher information density in both the spatial as well as the temporal dimension. The method provides quantitatively reasonable estimates of background concentrations, although the uncertainty at the hourly level is quite high. The main source of uncertainty is the low number of suitable background stations located in Norway. A major advantage of the technique is further that it can be easily updated with new data. Figure 3 shows an overview of typical annual average concentrations of NO_2 , O_3 , PM_{10} , and $\text{PM}_{2.5}$, as generated for the previous 2011 study.

While the methodology devised for the previous project provided reasonable estimates of background concentrations in Norway, both the spatial and temporal components are associated with significant uncertainties. Schneider et al. (2011) list several potential improvements for reducing the errors, among others they recommended the evaluation of auxiliary datasets such as satellite data and high-resolution model output. These datasets were evaluated here and the methodology and results are described in the following sections.

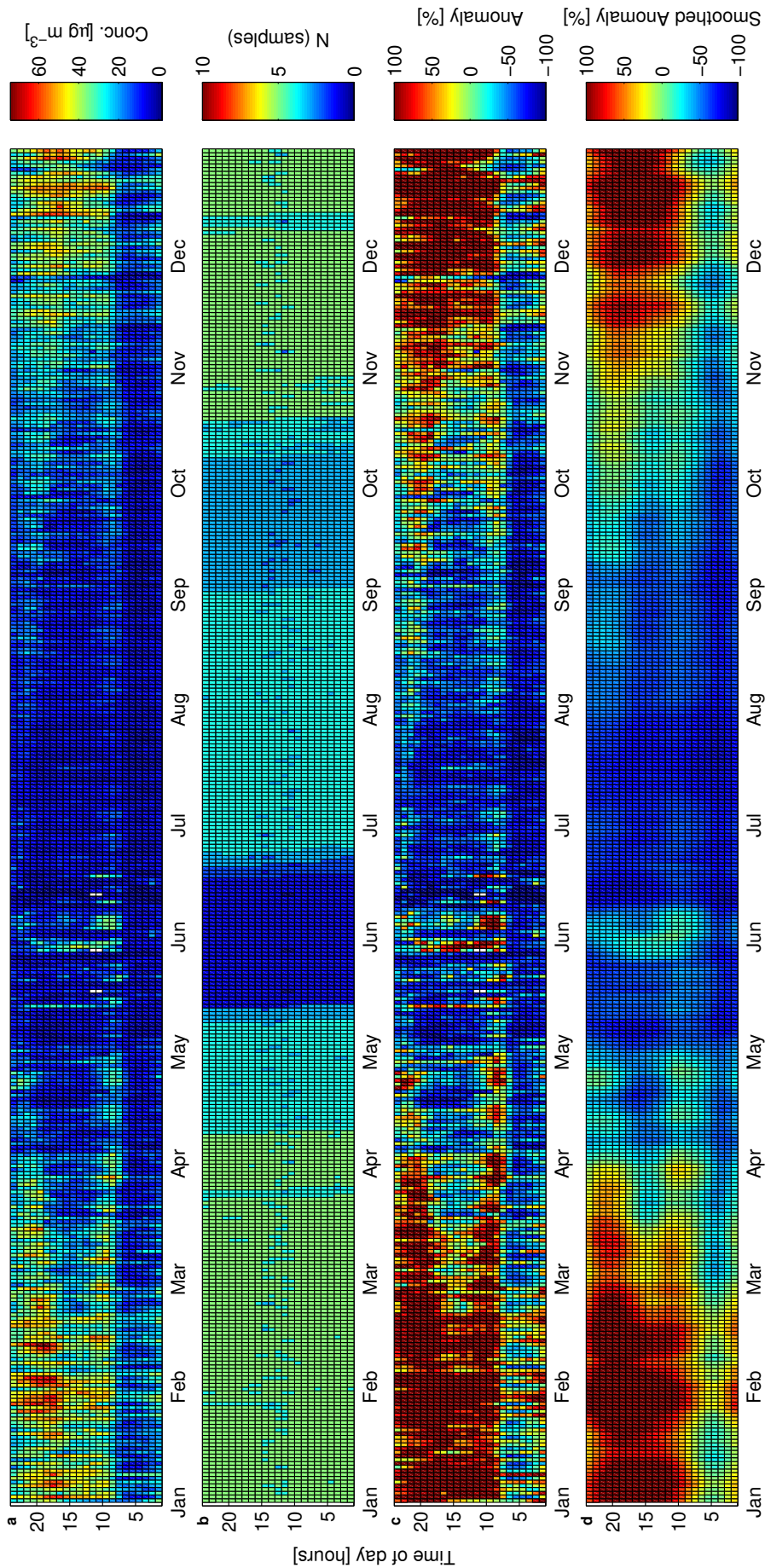


Figure 1 NO₂ at station NO0075A Barnebogen: Annual matrices of hourly averages computed over entire available time series, shown as a) Observations, b) number of years with available data, c) the anomaly computed from the long-term mean, and d) the anomaly from the long-term mean smoothed using a low-pass filter.

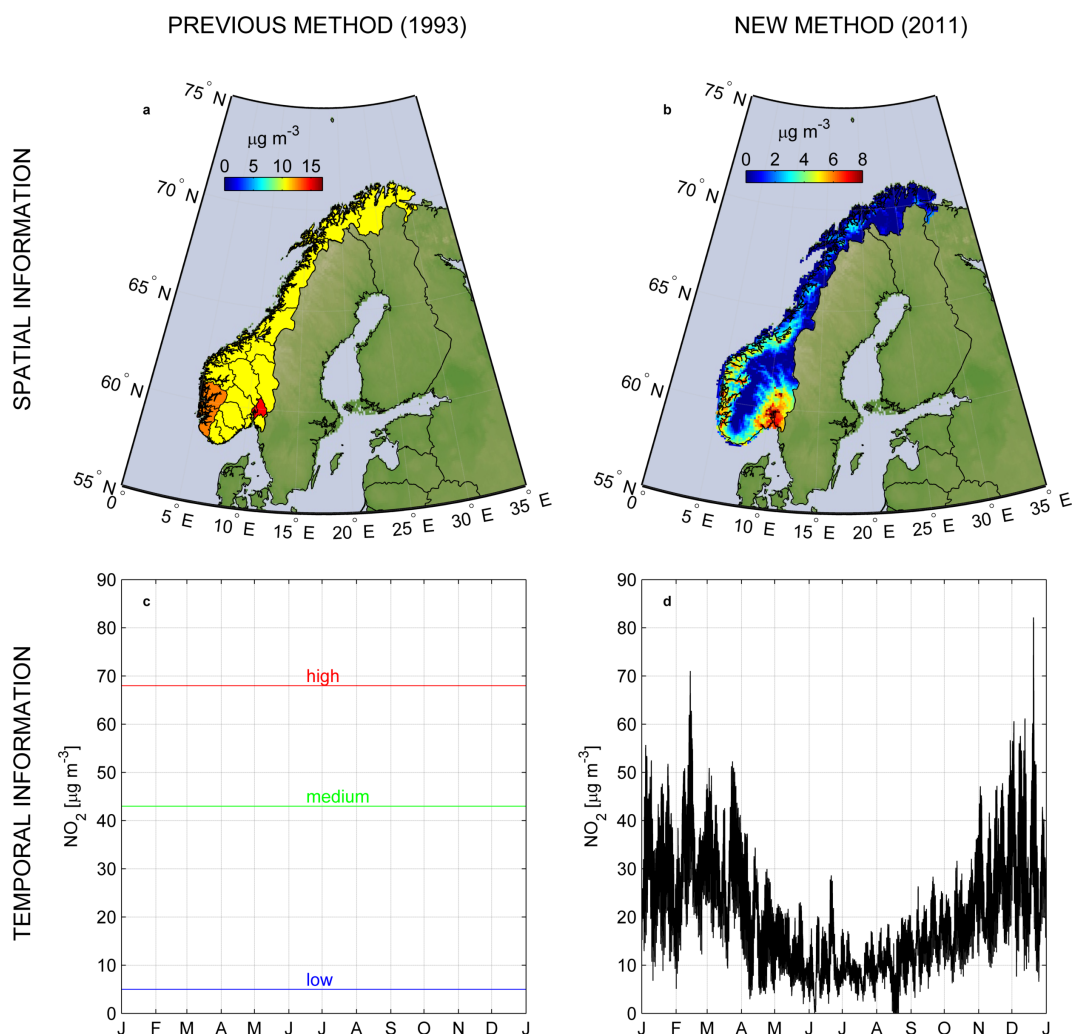


Figure 2 Comparison of the information content about background concentrations obtained from the previous method and the method described in this report, shown for the example of NO_2 . Panel a) shows 1993 VLUFT data for rural areas for the medium-level class, panel b) shows the annual mean background concentrations for 2008 derived using the method presented here, panel c) shows an example of temporal information available from VLUFT, here for Akershus county, and panel d) shows the temporal concentration information at Kjeller in Akershus country for a typical year as derived by the method presented here. Note that the values from VLUFT given in panel a) are "episodic high hourly concentrations" and are thus not directly comparable to the annual mean values shown in panel b). (From Schneider et al. (2011))

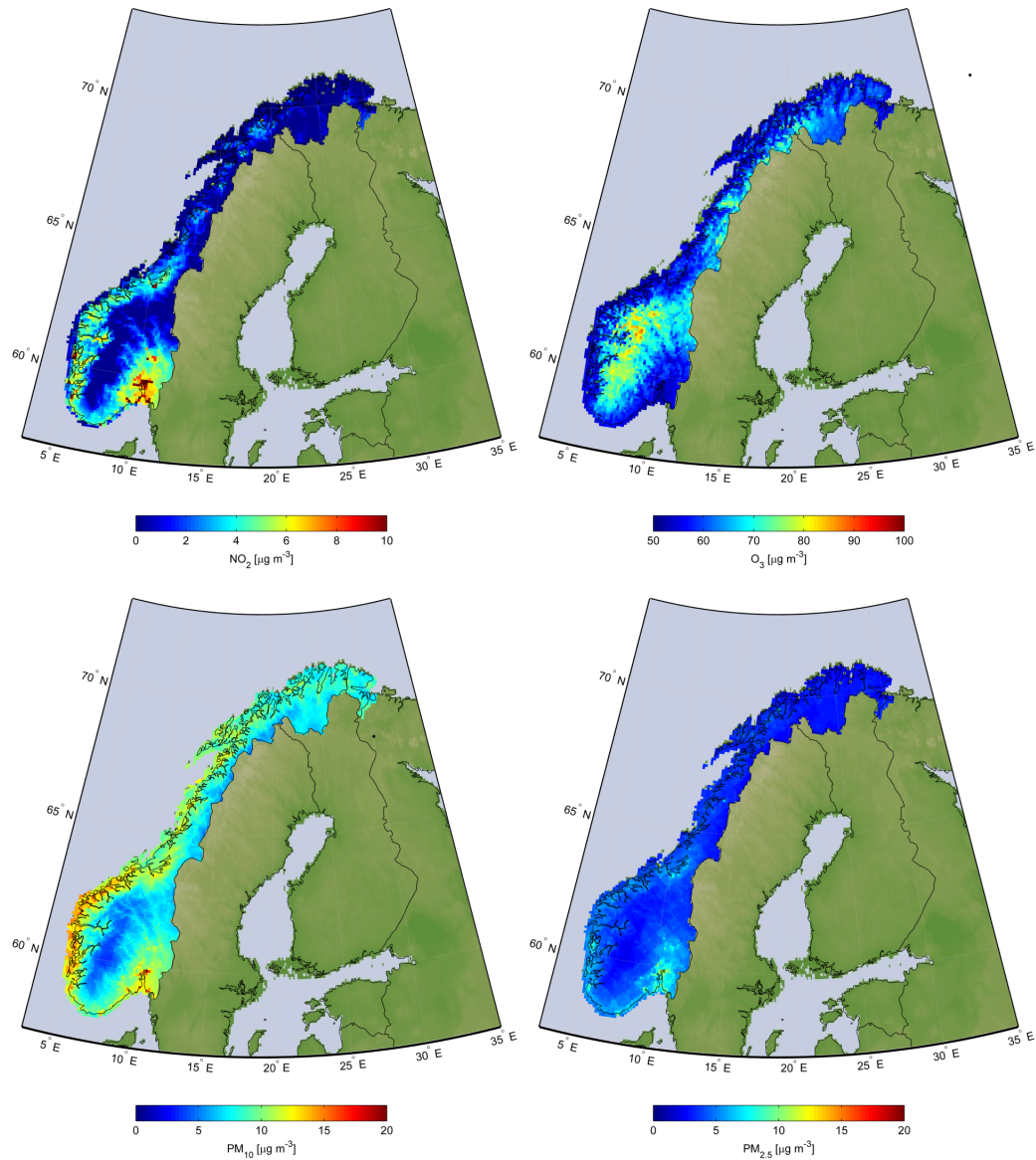


Figure 3 Maps of 2007 (NO_2) and 2008 annual means of NO_2 , O_3 , PM_{10} , and $\text{PM}_{2.5}$ as they were computed in the 2011 study. The spatial resolution of the grid is approximately $10 \text{ km} \times 10 \text{ km}$. The maps are partly based on data provided by the European Topic Centre on Air and Climate Change implementing a methodology described in Horálek et al. (2010). (From Schneider et al. (2011))

2 Data

A wide variety of data sources were used for this project. This includes hourly station data, satellite data, output from atmospheric chemistry models, and processed data from previous projects on mapping European air quality.

2.1 Station data

Raw data from air quality stations was used for both spatial mapping using residual kriging as well as for temporal decomposition of the time series. All station data was obtained from the *European Air quality dataBase*, AirBase (<http://acm.eionet.europa.eu/databases/airbase/>). However, different datasets were acquired for each component. For the geostatistical analysis, annual mean concentrations were acquired for all European background stations in order to achieve a large enough sample size for variogram modeling and regression analysis (see Figure 4). For the temporal characterization, only data for Norwegian stations were acquired for all four species, however this was done for the entire available record and at an hourly temporal resolution.

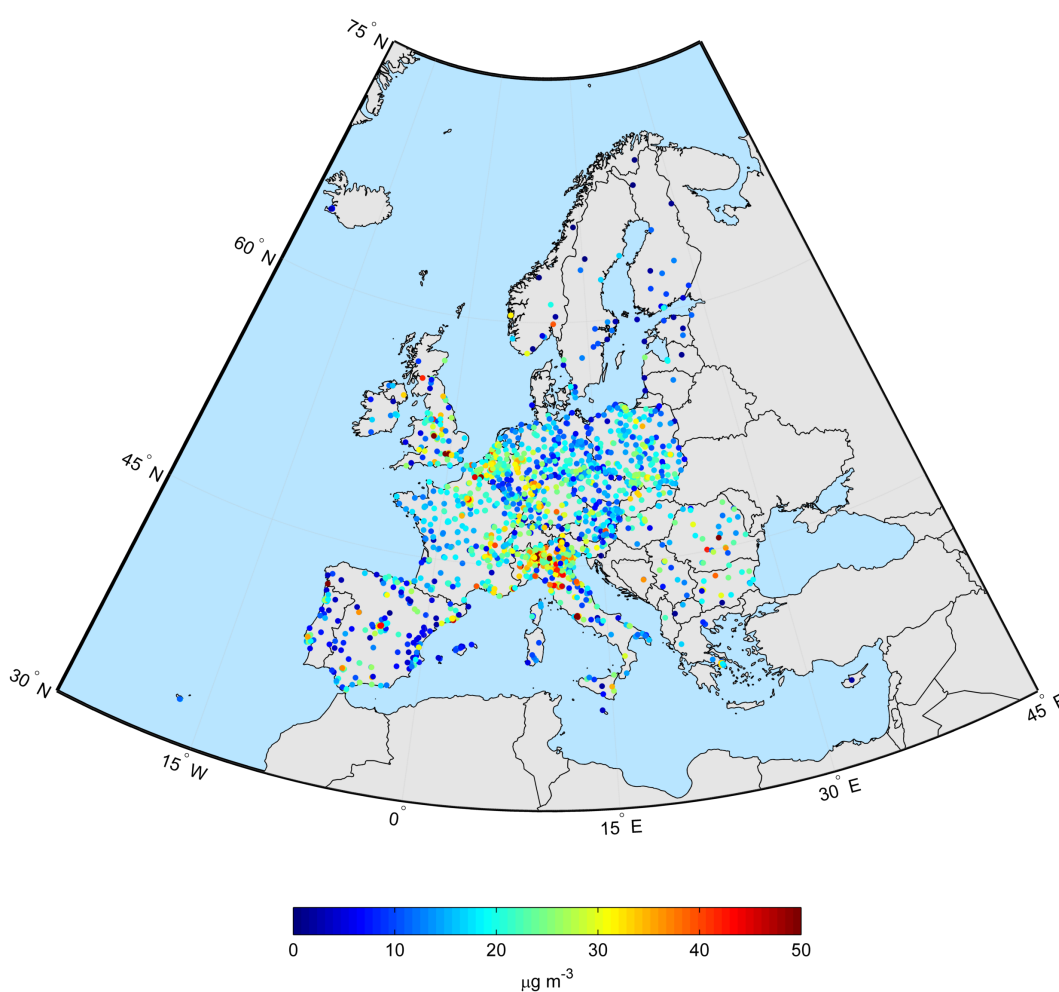


Figure 4 Map showing the 2009 average NO₂ concentration measured at all Airbase background stations. (from Schneider et al. (2011))

Table 1 lists all background air quality stations located in Norway for which data was retrieved for the temporal component from the AirBase database. Traffic and industrial stations were not used because of their limited spatial representativeness. Therefore, only background stations (urban, suburban, and rural) were considered. The geographical context is shown in Figure 5 which shows the location of all background air quality stations in Norway with suitably long time series for each component.

In addition, Table 2 gives an overview of station type and the components measured at each station with suitably long time series, as well as the respective long-term means for each component. Note that only a small number of stations provides suitable time series for NO₂ and only one station provides data for PM_{2.5}. Swedish and Finnish stations were not used here for the temporal characterization but could provide valuable additional information in future work.

2.2 Satellite NO₂ data

Operational satellite remote sensing of NO₂ has been carried out since 1995 when the Global Ozone Monitoring Experiment (GOME) (Burrows et al., 1999; Richter and Burrows, 2002) was first launched. Beginning in 2002, the observations were continued by the SCIAMACHY (SCanning Imaging Absorption spectroMeter for Atmospheric Cartography) sensor onboard of Envisat (Bovensmann et al., 1999; Gottwald et al., 2006), and subsequently complemented in 2004 by the Ozone Monitoring Instrument (OMI) (Levelt et al., 2006) as well as the Global Ozone Monitoring Experiment-2 (GOME-2) instrument in 2006 (Munro et al., 2006).

Two satellite datasets of NO₂ were evaluated here for their potential to be used within the context of European-scale air quality mapping. The first one was a monthly-averaged dataset acquired by the SCIAMACHY instrument and processed by the

Table 1 Overview of Norwegian background air quality stations that were used for temporal characterization. All station data was acquired from AirBase. Note that not all stations provide data for all air quality indicators and that stations not listed here were not considered due to short time series or other reasons. (from Schneider et al. (2011))

Station ID	Station Name	City	Lat. [deg]	Long. [deg]	Elevation [m]
NO0075A	Barnehaugen	LILLEHAMMER	61.121	10.467	210
NO0001R	Birkenes		58.383	8.250	190
NO0081A	Bærum		59.952	9.645	80
NO0070A	Grimmerhaugen	AALESUND	62.472	6.166	21
NO0077A	Gruben	MO I RANA	66.310	14.194	10
NO0062A	Haukenes		59.200	9.400	25
NO0056R	Hurdal		60.367	11.067	300
NO0045R	Jeløya		59.433	10.600	5
NO0055R	Karasjok		69.467	25.217	333
NO0039R	Kårvatn		62.783	8.883	210
NO0016A	Nedre Storgate	DRAMMEN	59.746	10.207	20
NO0041R	Osen		61.250	11.783	440
NO0043R	Prestebakke		59.000	11.533	160
NO0015A	Rådhuset	BERGEN	60.395	5.327	5
NO0052R	Sandve		59.200	5.200	40
NO0072A	Skøyen	OSLO	59.920	10.733	10
NO0073A	Sofienbergparken	OSLO	59.356	10.766	25
NO0063A	Stener Heyerdahl	KRISTIANSAND	58.090	7.586	12
NO0015R	Tustervatn		65.833	13.917	439
NO0065A	Våland	STAVANGER	58.961	5.731	33
NO0080A	Øyekast		59.133	9.645	40

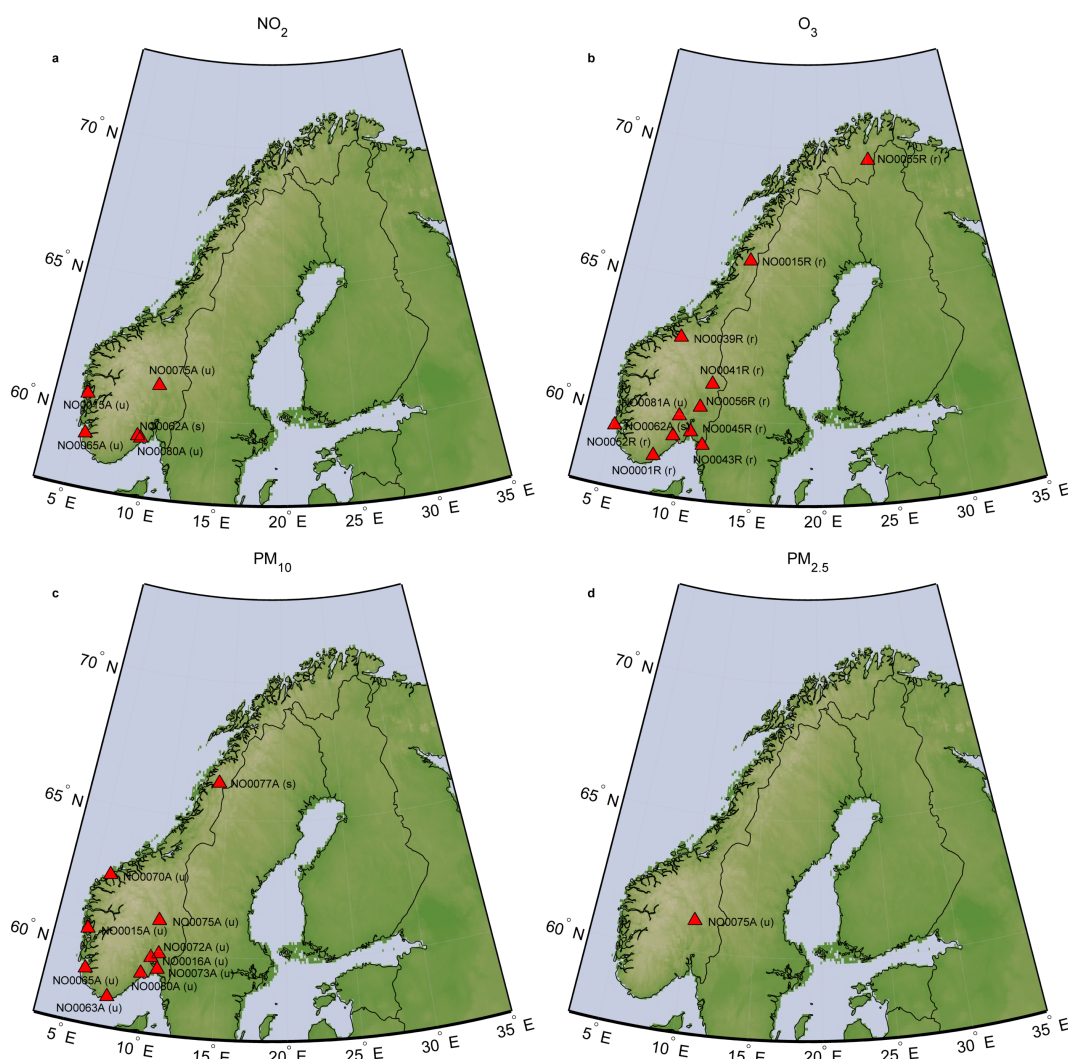


Figure 5 Location of the Norwegian background air quality stations whose data was used in this project for purposes of spatial mapping and temporal decomposition for a) NO_2 , b) O_3 , c) PM_{10} , and d) $\text{PM}_{2.5}$. The station type is indicated in the label as (u) for urban, (s) for suburban, and (r) for rural. Note that only stations with sufficiently long time series are shown.

Tropospheric Emission Monitoring Internet Service (TEMIS), which provides a comprehensive data archive at the website temis.nl. The retrieval algorithm used for the NO_2 product investigated here is based on the methodology developed by Boersma et al. (2011) and is described in more detail in Section 3.1. Monthly global NO_2 data for the entire lifetime of the SCIAMACHY instrument was available but only 2009 data has been used for comparison purposes here.

The second dataset tested here was acquired by the OMI instrument which flies onboard of NASA's Aura platform. The specific dataset used was an experimental high-resolution product based on the OMNO2e Level 3 product. This dataset is produced at NASA Goddard based on the retrieval algorithm described by Bucsela et al. (2006) and Bucsela (2012). Global NO_2 data with a daily sampling rate for the entire year of 2009 was available for this dataset.

Detailed information about the respective retrieval algorithms of the two satellite-based NO_2 products are given in Section 3.1.

Table 2 Overview of station type and components measured at each station as well as their respective long-term mean. All means are given in units of $\mu\text{g m}^{-3}$. When no annual mean is indicated the data either did not have sufficiently long time series for computing annual and daily means or the component was not measured at that station. The column CHIMERE indicates whether the station is located within the extent of the CHIMERE model output and thus is suitable for model comparisons. (from Schneider et al. (2011))

Station ID	Station Name	Type	CHIMERE	NO ₂	O ₃	PM ₁₀	PM _{2.5}
NO0075A	Barnehaugen	urban	yes	19.2	-	19.0	8.8
NO0001R	Birkenes	rural	no	-	55.2	-	-
NO0081A	Bærum	urban	yes	-	39.0	-	-
NO0070A	Grimmerhaugen	urban	no	-	-	13.1	-
NO0077A	Gruben	suburban	no	-	-	17.4	-
NO0062A	Haukenes	suburban	yes	5.6	54.8	-	-
NO0056R	Hurdal	rural	yes	-	54.6	-	-
NO0045R	Jeløya	rural	yes	-	56.1	-	-
NO0055R	Karadjok	rural	no	-	65.7	-	-
NO0039R	Kårvatn	rural	no	-	58.6	-	-
NO0016A	Nedre Storgate	urban	yes	-	-	19.9	-
NO0041R	Osen	rural	yes	-	55.8	-	-
NO0043R	Prestebakke	rural	yes	-	58.5	-	-
NO0015A	Rådhuset	urban	yes	34.7	-	17.9	-
NO0052R	Sandve	rural	yes	-	66.2	-	-
NO0072A	Skøyen	urban	yes	-	-	21.8	-
NO0073A	Sofienbergparken	urban	yes	-	-	22.0	-
NO0063A	Stener Heyerdahl	urban	yes	-	-	22.1	-
NO0015R	Tustervatn	rural	no	-	70.0	-	-
NO0065A	Våland	urban	yes	16.7	-	15.8	-
NO0080A	Øyekast	urban	yes	14.5	-	17.1	-

2.3 ETC/ACM data

As previously described in Schneider et al. (2011), existing data sets generated by the European Topic Centre on Air Pollution and Climate Change Mitigation (ETC/ACM) were used for the mapping component, whenever possible. The methodology underlying the mapping procedure has been refined over many years and the datasets have been extensively validated (Horálek et al., 2007, 2010; Denby et al., 2011). Such data was available for NO₂, PM₁₀, and PM_{2.5}, however not for O₃. The annual average map for O₃ over Norway was produced at NILU from raw datasets using a similar methodology.

The mapping methodology used by the ETC/ACM is described in detail in various reports, such as Horálek et al. (2007), Horálek et al. (2010), and Denby et al. (2011), and therefore will only be summarized here briefly. The approach uses a combination of a linear regression model which is then followed by the kriging of the resulting residuals, a process also known as residual kriging (Goovaerts, 1997). Separate maps are created for urban and rural areas which are later combined using specific merging rules based on population density. For each species and mapping type, a varying number of spatially exhaustive auxiliary variables are used which guide the interpolation process in areas of low station density. The type and number of auxiliary variables used within the mapping procedure is dependent on their respective impact to an improved fit of the regression model. For example, the interpolation of PM₁₀ in rural areas used output from the EMEP model, a digital elevation model for information on altitude, data on wind speed, and data on solar radiation. On the other hand, for PM₁₀ mapping in urban areas the used auxiliary variables consisted solely of the output from the EMEP model. For more detail on the auxiliary variables

used for the mapping of NO_2 , PM_{10} , and $\text{PM}_{2.5}$ see the reports provided by Horálek et al. (2007), Horálek et al. (2010) and Denby et al. (2011).

Once the multiple linear regression against the appropriate auxiliary variables is accomplished, residuals are acquired at each location where station data is available. These residuals are subsequently interpolated using ordinary kriging (Cressie, 1993; Goovaerts, 1997; Wackernagel, 2003). This interpolation process is based on variogram analysis, according to which the spatial autocorrelation of the data is fitted using a (often spherical) variogram model. Kriging weights are obtained as a result of this process and the optimal prediction of residual concentration is made at each $10 \text{ km} \times 10 \text{ km}$ grid cell. Subsequently, a final map of estimated concentrations is obtained by adding the gridded result from the linear regression and from the kriging of the residuals.

In addition to the linear regression and ordinary kriging techniques resulting in estimated concentration maps for rural and urban areas, the ETC/ACM methodology further uses a fairly sophisticated merging procedure for combining the separately interpolated maps of urban and rural areas. The technique is based on the population density for each grid cell and assign the interpolated value from the rural map if the population density is less than a given threshold α_1 and assigns the interpolated urban value for all cells exceeding a population density of α_2 . In case the population density is greater than α_1 but less than α_2 , a joint rural/urban value is computed using a weighting function and assigned to the respective grid cell. Once all the grid cells are assigned their appropriate concentration values based on their respective population density, a final concentration map of the parameter in question is obtained.

2.4 CHIMERE Model Data

A one-year high-resolution run of the three-dimensional chemistry-transport model CHIMERE (Schmidt et al., 2001; Vautard et al., 2001; Vautard, 2003; Bessagnet et al., 2004) was used for this part of the study.

Originally developed as an extension of a regional-scale model developed for the Paris area (Vautard et al., 2001), CHIMERE is a multi-scale chemical transport model which is primarily designed to generate daily forecasts of ozone, aerosols and other pollutants, as well as for producing long-term simulations for the purpose of emission control scenarios.

Europe-wide CHIMERE output for the entire year 2009 with an hourly sampling rate and a spatial resolution of $0.0625^\circ \times 0.125^\circ$ (approximately $7 \text{ km} \times 7 \text{ km}$) was available for this study. Unfortunately, the northernmost extent of the model domain was 61.8°N , which does not include all of Norway. However, most of southern Norway, which includes Norway's two largest urban areas Oslo and Bergen is included in the model domain. It was therefore decided to go ahead and test the methodology based on this region even though it was not possible to integrate the dataset in the operational mapping procedure for all of Norway.

3 Methodology

3.1 Satellite Retrieval Methodology

Two satellite NO₂ products were further investigated for their potential use within this study. The first product tested was acquired by the SCIAMACHY instrument onboard of the Envisat platform. The product used is based on the TEMIS retrieval algorithm (Boersma et al., 2011).

In short, the TEMIS NO₂ retrieval is based on three steps: The first step of the algorithm consists of a Differential Optical Absorption Spectroscopy (DOAS) retrieval of the total slant column of NO₂ from the measured spectrum, where absorption cross sections of NO₂, ozone, H₂O as well as a synthetic ring spectrum are taken into account, and a fifth order polynomial is included in the fit to account for scattering effects. The second step consists of the separation of the stratospheric and tropospheric NO₂ contributions to the total NO₂ column, where the stratospheric NO₂ column is estimated by assimilating total slant columns in the TM4 chemistry transport model (Dentener et al., 2003; Boersma et al., 2007). The third and final step of the retrieval is the conversion of the tropospheric NO₂ slant columns into vertical columns using a calculated Air-Mass Factor (AMF). Further details on the specific retrieval methodology can be found in Boersma et al. (2004), Boersma et al. (2007), and Boersma et al. (2011), as well as on the TEMIS website (www.temis.nl).

Solely data reprocessed with version 2.0 of the retrieval algorithm was used. Improvements in version 2.0 over previous versions of the retrieval algorithm include an updated albedo database, a modified calculation of the air mass factor, a correction of the surface height calculation, a correction of the weekly cycle in NO_x emissions, as well as an increased number of NO_x tracers in the applied chemical transport model (Boersma et al., 2011). The NO₂ dataset used here only considered cloud radiance fractions of less than 50%. It was also resampled from the original SCIAMACHY spatial resolution to a 0.25 degree × 0.25 degree grid.

Although the TEMIS-based NO₂ dataset used in this study is based to some extent on data assimilation using the TM4 model (Dentener et al., 2003; Boersma et al., 2007), it is almost independent of the used emission inventory due to the retrieval set-up. The data assimilation results are mainly used to provide the stratospheric NO₂ column in the second step. This stratospheric column is virtually independent of the used emission database. For the calculation of the AMF in the third step knowledge of the profile shape of the vertical NO₂ distribution is needed. This profile shape is also taken from the data assimilation. However, the profile shape is independent of the emissions, since the data assimilation is scaling the NO₂ column with conservation of the shape. In conclusion, the NO₂ data are considered as retrieval results independent of emission data.

The second satellite NO₂ product tested here was acquired by the Ozone Mapping Instrument onboard the Aura satellite. The OMI product used within the framework of this study is based on a retrieval algorithm developed at NASA (Chance, 2002). The original, version 1 retrieval algorithm is described in Bucsele et al. (2006). The new version 3.0 retrieval algorithm is greatly improved over the previous versions (Bucsele, 2012).

The retrieval algorithm for the OMI NO₂ product consists of a total number of four major steps: A Differential Optical Absorption Spectroscopy, a calculation of the

air mass factor, destriping, and a troposphere-stratosphere separation. The DOAS analysis first divides earthshine radiances by the reference solar irradiance spectrum. The normalized spectra are then fitted to trace gas spectra observed in the laboratory using a reference Ring spectrum and a polynomial function. The DOAS fitting is applied in the spectral range of 405 nm to 465 nm. In a next step, the air mass factor is calculated using scattering weights and a monthly mean climatology of NO₂ profile shapes, which were derived from a chemical transport model. The AMF is subsequently computed using the cloud radiance fraction f as

$$AMF = (1 - f) \cdot AMF_{clear} + f \cdot AMF_{cloud} \quad (1)$$

where AMF_{clear} and AMF_{cloud} are the model-derived air mass factors for clear and cloudy conditions, respectively. Following the AMF calculation, the NO₂ slant column densities observed by OMI are then “destriped” in order to correct for an instrument artifact. Finally, as a fourth step, a troposphere-stratosphere separation is performed using an *a priori* estimate of the tropospheric contribution based on a monthly model climatology.

More information about the OMI NASA retrieval algorithm can be found in Bucsele et al. (2006), Bucsele (2012), and OMI Team (2012). The OMINO2 product (Chance, 2002) is estimated to have a fitting error in the slant column of approximately $0.3 - 1 \times 10^{15}$ molecules cm⁻² (OMI Team, 2012).

3.2 Geostatistical framework

The European background maps are created using a geostatistical technique, namely residual kriging with auxiliary variables. Kriging is an interpolation technique that makes use of a model of spatial autocorrelation (usually in the form of a variogram model) to infer optimal estimates of a variable at a given set of locations (Isaaks and Srivastava, 1989; Cressie, 1993; Goovaerts, 1997; Wackernagel, 2003).

The mapping procedure applied in this study is based on the previous work by Horálek et al. (2007), Horálek et al. (2010), and Denby et al. (2011) and involves a linear regression analysis against an auxiliary variable in conjunction with kriging of the residuals. It should be noted that the cited work incorporates a procedure for separately mapping urban and rural areas and then combining the interpolated maps using a merging technique. This part of the algorithm was not implemented in the mapping procedure for this project.

The concentration $\hat{Z}(s_0)$ is mapped at a given location s_0 using the model

$$\hat{Z}(s_0) = c + a_1X_1(s_0) + a_2X_2(s_0) + \dots + a_nX_n(s_0) + \eta(s_0) \quad (2)$$

where $c, a_1, a_2 \dots a_n$ are parameters of the multiple linear regression and $X_1(s_0) \dots X_n(s_0)$ are the values of the auxiliary variables used at location s_0 . Finally, $\eta(s_0)$ represents the results of the ordinary kriging of the residuals at location s_0 . While equation 2 provides a general methodology for incorporating multiple auxiliary variables, only single auxiliary variables were tested here in order to evaluate the impact of each auxiliary variable individually (with one exception mentioned later on). The first step in the process was therefore to establish a linear relationship between the annual average NO₂ concentration at each station and the respective auxiliary variable at each station. This task was performed throughout all background stations in Europe available within AirBase (with exception of those stations used for validation) in order to obtain a representative relationship.

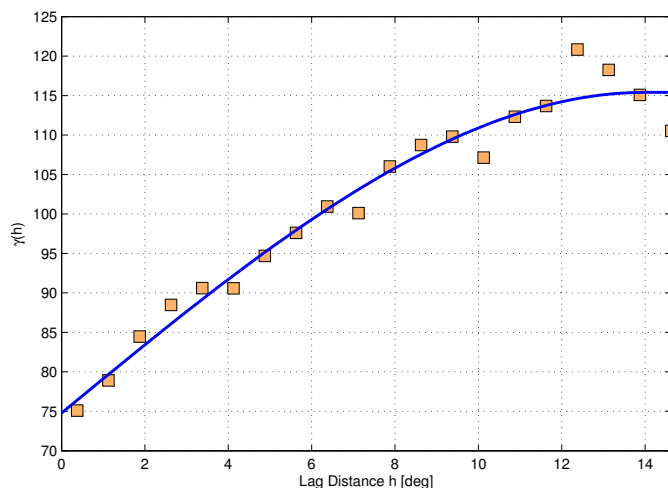


Figure 6 Example of an empirical semivariogram $\hat{\gamma}(h)$ and its model, describing the autocorrelation of a European NO₂ station dataset. The model in this case is a combination of a nugget effect of 74.7 and a spherical model with sill 40.6 and a range of 14 degrees.

Kriging makes use of a model describing the spatial autocorrelation. Most often, the semivariogram $\gamma(h)$ at a certain lag distance h is used to describe this. Different types of models are then fitted to the empirical semivariogram, with a spherical and Gaussian models probably being the most common. Figure 6 shows an example of the empirical semivariogram and the fitted spherical model used for residual kriging of NO₂ over Europe.

For kriging of residuals, a model was fitted to the empirical semivariogram of the residuals with a combination of a nugget effect model and a spherical or Gaussian model of range a_0 degrees and sill $c_0 \mu\text{g m}^{-3}$ such that the semivariance $\hat{\gamma}$ at lag h is given as either

$$\hat{\gamma}(h) = \begin{cases} c_0 \cdot \left[\frac{3}{2} \frac{h}{a_0} - \frac{1}{2} \left(\frac{h}{a_0} \right)^3 \right] & \text{for } h \leq a_0 \\ c_0 & \text{for } h > a_0 \end{cases} \quad (3)$$

for the spherical model or

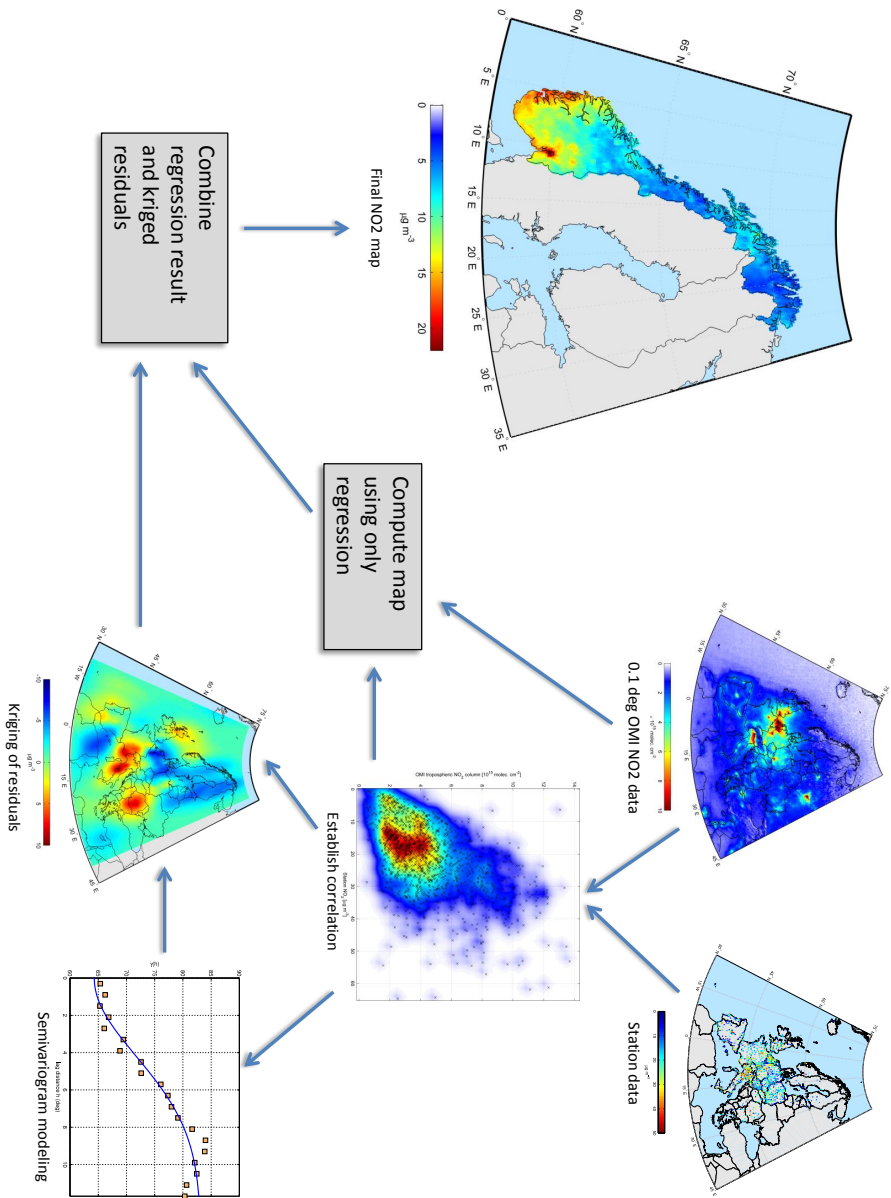
$$\hat{\gamma}(h) = c_0 \left[1 - \exp\left(-\frac{h^2}{a_0^2}\right) \right] \quad (4)$$

for the Gaussian model.

The fitted semivariogram model is then used in the kriging process to determine appropriate weighting factors for each data point. More detailed information about the kriging process can be found in the literature, e.g. in Isaaks and Srivastava (1989), Cressie (1993), or Goovaerts (1997). The kriged residuals are then added to the results from the multiple linear regression as indicated in Equation 2 and through this process the final results are obtained.

Figure 7 illustrates the basic workflow using a schematic of the methodology for the case of using satellite data as an auxiliary variable.

Figure 7 Schematic of the general methodology, here illustrated on the example of using OMI NO₂ satellite data as an auxiliary dataset for kriging station observations of NO₂.



4 Results and Discussion

In the following sections the results of the three main tasks of this project are presented and the implications discussed. First, the impact of integrating satellite data of NO₂ in the mapping procedure is described. Subsequently, the potential of high-resolution output of a chemical transport model is evaluated. Finally, a web-based mapping tool for visualizing and accessing the spatial and temporal information in the dataset of background concentrations over Norway is presented.

4.1 NO₂ mapping in Norway using satellite data

Based on a growing importance of spaceborne data for air quality related applications it is highly desirable to study the impact of satellite data on currently existing air quality mapping techniques. In this section, the potential of using satellite-based NO₂ data as an auxiliary variable for mapping air quality at the European and Norwegian scale using geostatistical techniques is investigated. Two satellite products were compared and one was selected for further use within the actual mapping procedure.

4.1.1 Choosing a suitable satellite product

As a first objective of this task, a satellite product suitable for use within the mapping procedure had to be found. For this purpose, two satellite-based NO₂ products were chosen for further investigation: The SCIAMACHY product based on the algorithm by TEMIS (Boersma et al., 2011), and the OMNO2e product (Bucsela et al., 2006; Bucsela, 2012). Figures 8 and 9 show the 2009 annual mean tropospheric NO₂ columns derived from the OMI and SCIAMACHY products, respectively, each using different retrieval algorithms. Note that the color scale on both figures is identical, so both qualitative and quantitative comparisons can be carried out.

Overall, the spatial patterns shown by the two products agree quite well. All the major regions of generally high NO₂ concentrations, such as the region of Belgium and the Netherlands, southern and eastern England, as well as the Po valley region in Northern Italy, are captured adequately by both products. Furthermore, individual NO₂ hotspots over more isolated cities such as Moscow, Madrid, and Istanbul are easily identifiable from both data products. The map produced from OMI data appears to be slightly smoother whereas the SCIAMACHY-based maps shows a bit more “noise”. This is due to the fact that the OMI-based annual mean map was computed by averaging over daily images, whereas the SCIAMACHY-based annual mean was calculated from monthly average datasets, which in turn were derived from daily data.

In terms of actual NO₂ concentrations, it is obvious from the two figures that SCIAMACHY overall measures significantly higher columns in the polluted areas than OMI. Figure 9 clearly shows this effect as significantly larger areas exceeding 10×10^{15} molecules cm⁻² as compared to 8. This effect is particularly obvious in the Po valley region in Northern Italy, for which the OMI annual mean only shows very few grid cells exceeding 10×10^{15} molecules cm⁻², whereas most of the region of Northern Italy exceeds this value in the SCIAMACHY-based map.

The reason for this behavior can be found in the combination of the strong diurnal cycle of NO₂ in heavily polluted areas and the different overpass times of the two

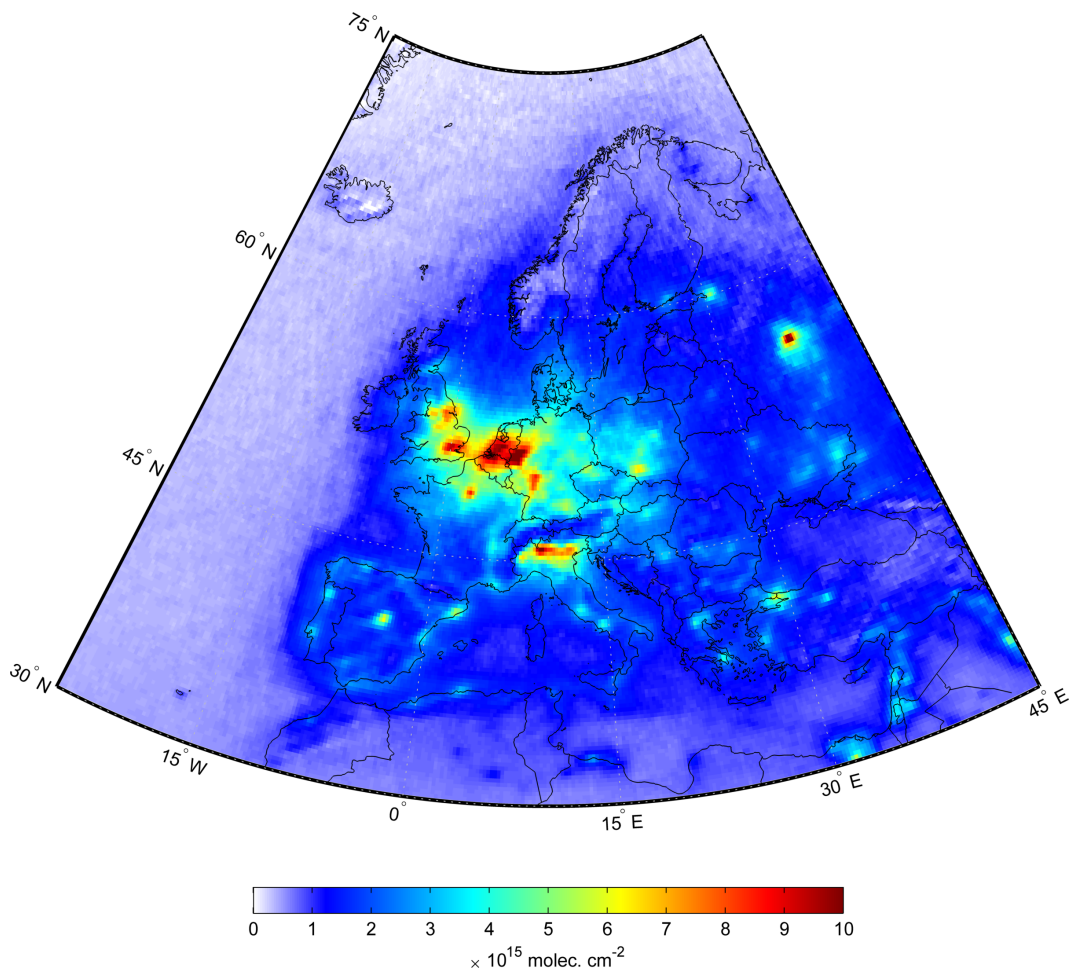


Figure 8 Annual mean NO_2 concentration for the year 2009 derived from the OMNO2e daily $0.25^\circ \times 0.25^\circ$ product. Note that the overpass time of the Aura platform on which OMI is flying, is at approximately 13:30 local time.

instruments. While the Envisat satellite, on which the SCIAMACHY instrument is mounted, has a local overpass time at the equator of around 10:00 local solar time (LST), and thus samples the tail end of the morning rush hour, the OMI instrument on the Aura platform has a local overpass time at the equator of approximately 13:45 LST and as such samples the atmosphere in the middle between the morning and evening rush hours. As such, its observations of tropospheric NO_2 columns are expected to be lower than those obtained from SCIAMACHY.

In order to explore the quantitative difference between the two products in more detail and with a particular focus on spatial patterns, a difference image between the products from the two instruments was produced. The difference in NO_2 column ΔC given in $\times 10^{15}$ molecules cm^{-2} was calculated as

$$\Delta C = C_{\text{SCIAMACHY}} - C_{\text{OMI}} \quad (5)$$

where $C_{\text{SCIAMACHY}}$ and C_{OMI} are the annual mean NO_2 column for SCIAMACHY and OMI, respectively. Based on this equation, positive values in the difference image indicate that the SCIAMACHY retrieval is higher than the OMI retrieval, and negative values indicate the opposite.

Figure 10 shows the resulting difference map. As expected, the highest absolute differences can be found over the most highly polluted areas. In Northern Italy, which

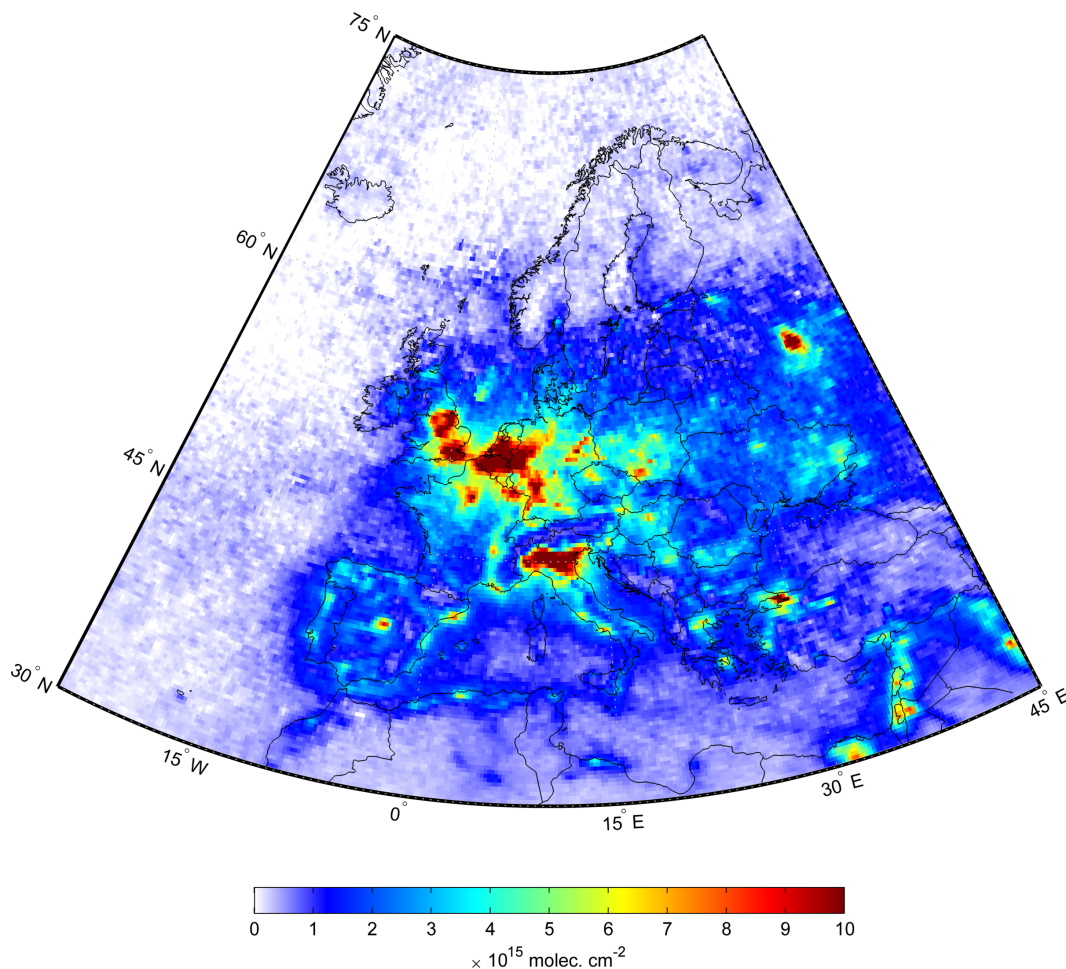


Figure 9 Annual mean NO₂ concentration for the year 2009 derived from the SCIAMACHY/TEMIS monthly $0.25^\circ \times 0.25^\circ$ product. Note that the overpass time of the Envisat platform on which SCIAMACHY is flying, is at approximately 10:00 local time.

exhibits the largest area of substantial differences, the values easily reach and exceed 5×10^{15} molecules cm^{-2} . Several regions in Germany, Belgium, the Netherlands, and the United Kingdom also reach such high values, albeit only in areas of considerably smaller spatial extent. SCIAMACHY generally shows higher tropospheric columns by approximately 1×10^{15} molecules cm^{-2} on average over large areas of Eastern Europe, particularly in the Ukraine.

In areas of generally low tropospheric NO₂ concentrations such as over the oceans, Scandinavia, and Africa, OMI exhibits slightly higher values by approximately 0.5×10^{15} molecules cm^{-2} . However, this magnitude is easily within the error range specified for the products and thus probably is not of too much significance.

It should be noted that, while such an inter-comparison between two satellite products is not a substitute for validation with in situ data as it can not provide an absolute error estimate, it can provide valuable information on spatial patterns in differences.

Despite differences in absolute values, it is critical to point out that the spatial patterns indicated by both instruments are very consistent. This is important because when using such satellite-based maps as an auxiliary datasets for supporting kriging of station data, it is primarily the spatial patterns that have an impact on the results, whereas the absolute values are based on the station data.

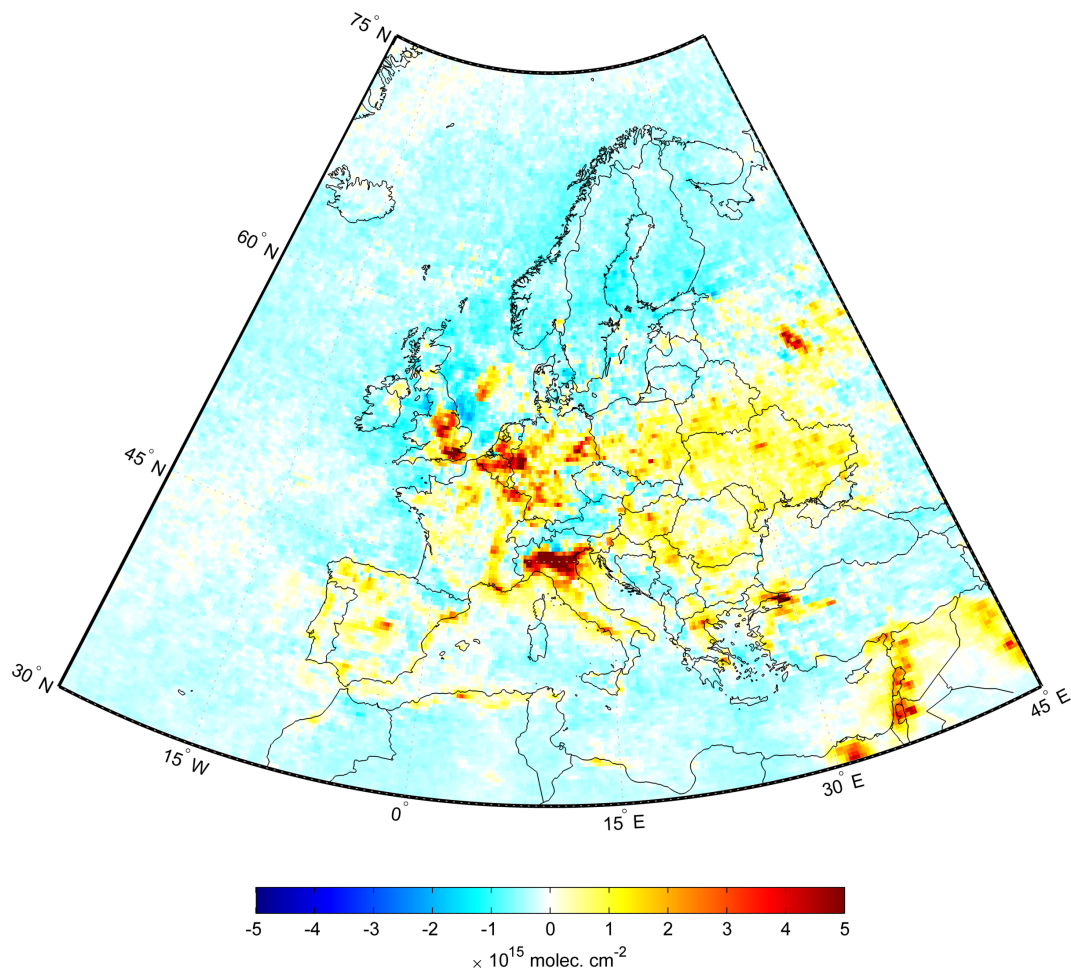


Figure 10 Difference image of the mean annual NO_2 column retrieved from SCIAMACHY and OMI. The difference is calculated based on Equation 5. Note that both satellite instruments have significantly different overpass times (10:00 vs. 13:30 local time), which together with the diurnal cycle of NO_2 explain the majority of the inter-sensor biases.

While for the previous figures and analysis the $0.25^\circ \times 0.25^\circ$ resolution OMI product was used to provide as much consistency as possible with the SCIAMACHY product, a high-resolution $0.1^\circ \times 0.1^\circ$ OMNO2e product exists for the OMI instrument. Given the similarity in spatial scale between the $0.1^\circ \times 0.1^\circ$ OMNO2e product and the 10 km spatial resolution at which air quality is being mapped operationally in Europe by the ETC/ACM, this product is a natural choice for this study. Figure 12 shows a direct comparison of the two OMI products. The high resolution product clearly can resolve more detail and provides higher values in some hotspots which do not appear in the $0.25^\circ \times 0.25^\circ$ resolution product due to spatial averaging.

Based on these results and further based on the fact that a $0.1^\circ \times 0.1^\circ$ product was available from OMI while only $0.25^\circ \times 0.25^\circ$ resolution was available from SCIAMACHY, it was decided to use the OMNO2e product for the remainder of this study. The relatively high resolution of the OMNO2e product allows for mapping at the 10 km grid cell level for all of Europe. It should further be noted that, in contrast to for example SCIAMACHY data, OMI observations are available at present and further will be continued at an even higher spatial resolution in 2014 with the launch of the TROPOMI instrument onboard the Sentinel-5 precursor platform.

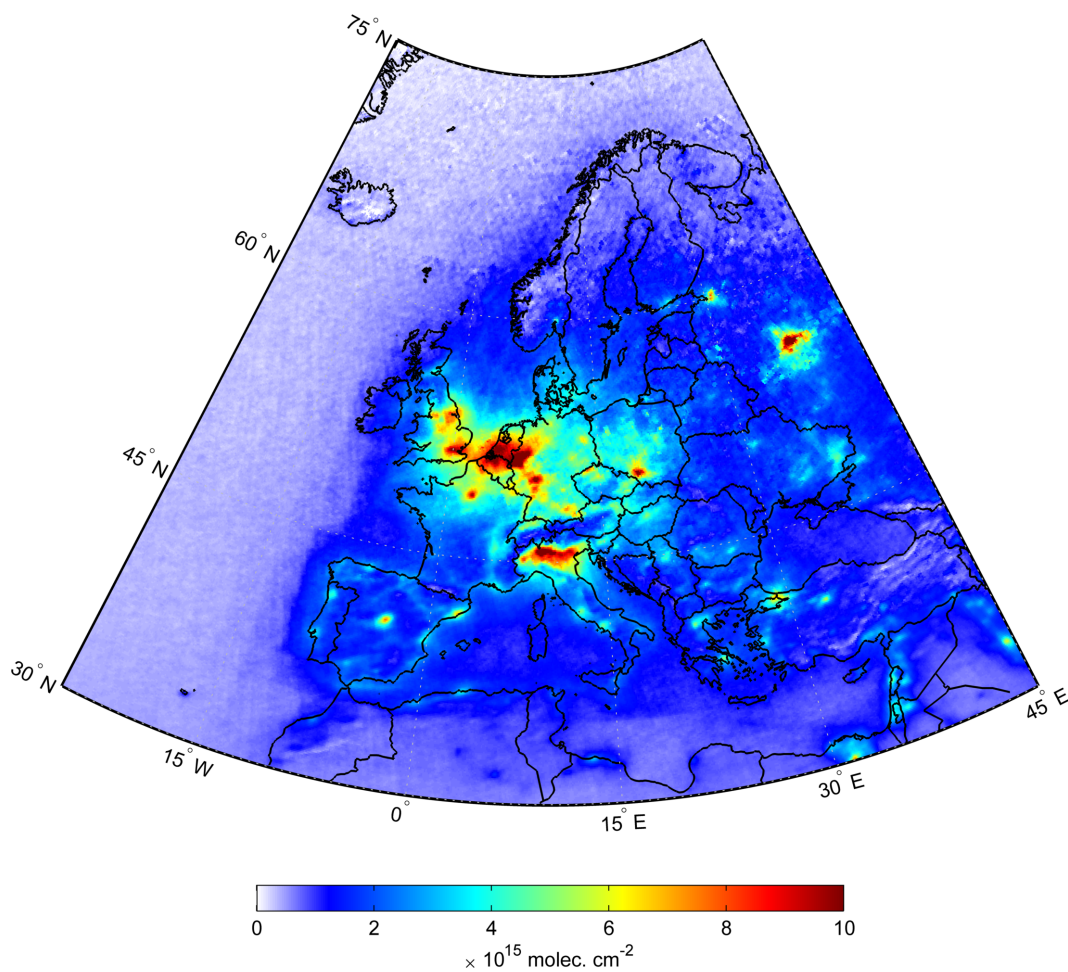


Figure 11 The $0.1^\circ \times 0.1^\circ$ resolution OMNO2e product over Europe. Shown here is the 2009 annual mean tropospheric NO₂ concentration. Significantly more detail is visible than in the standard resolution product (see also Figure 12). See also the same figure with adjusted extent and color scale showing Norway only (Figure 13).

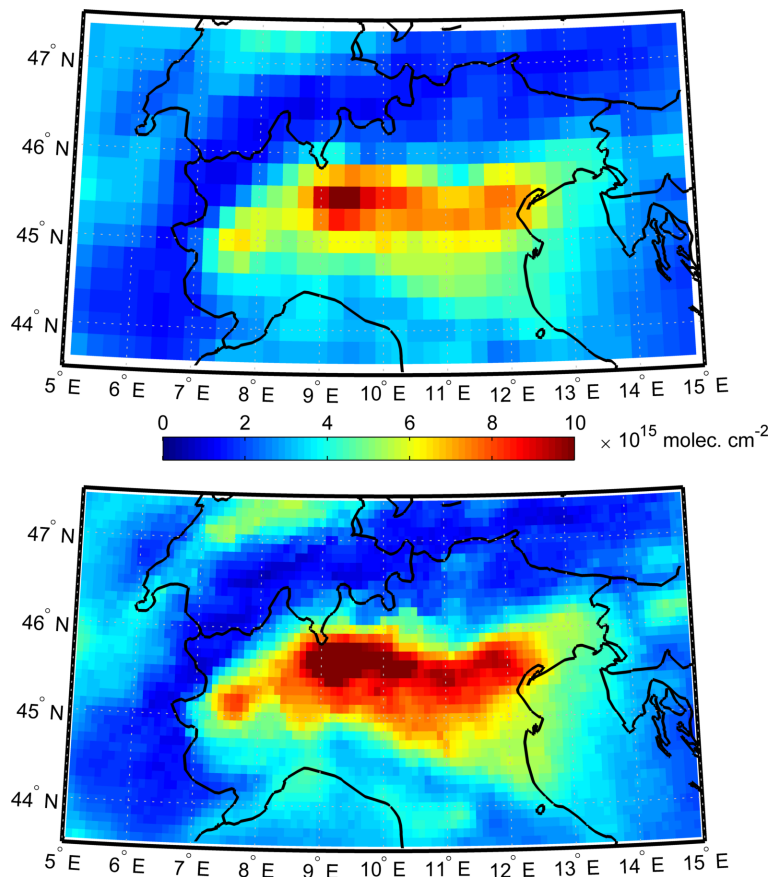


Figure 12 Comparison of the $0.25^\circ \times 0.25^\circ$ resolution OMNO2e product (top) with the 0.1 degree resolution OMNO2e product (bottom), shown for the Po valley region in Northern Italy. The higher resolution product clearly shows details not visible in the image of the $0.25^\circ \times 0.25^\circ$ resolution product. The figures show the annual mean tropospheric NO₂ column in 2009.

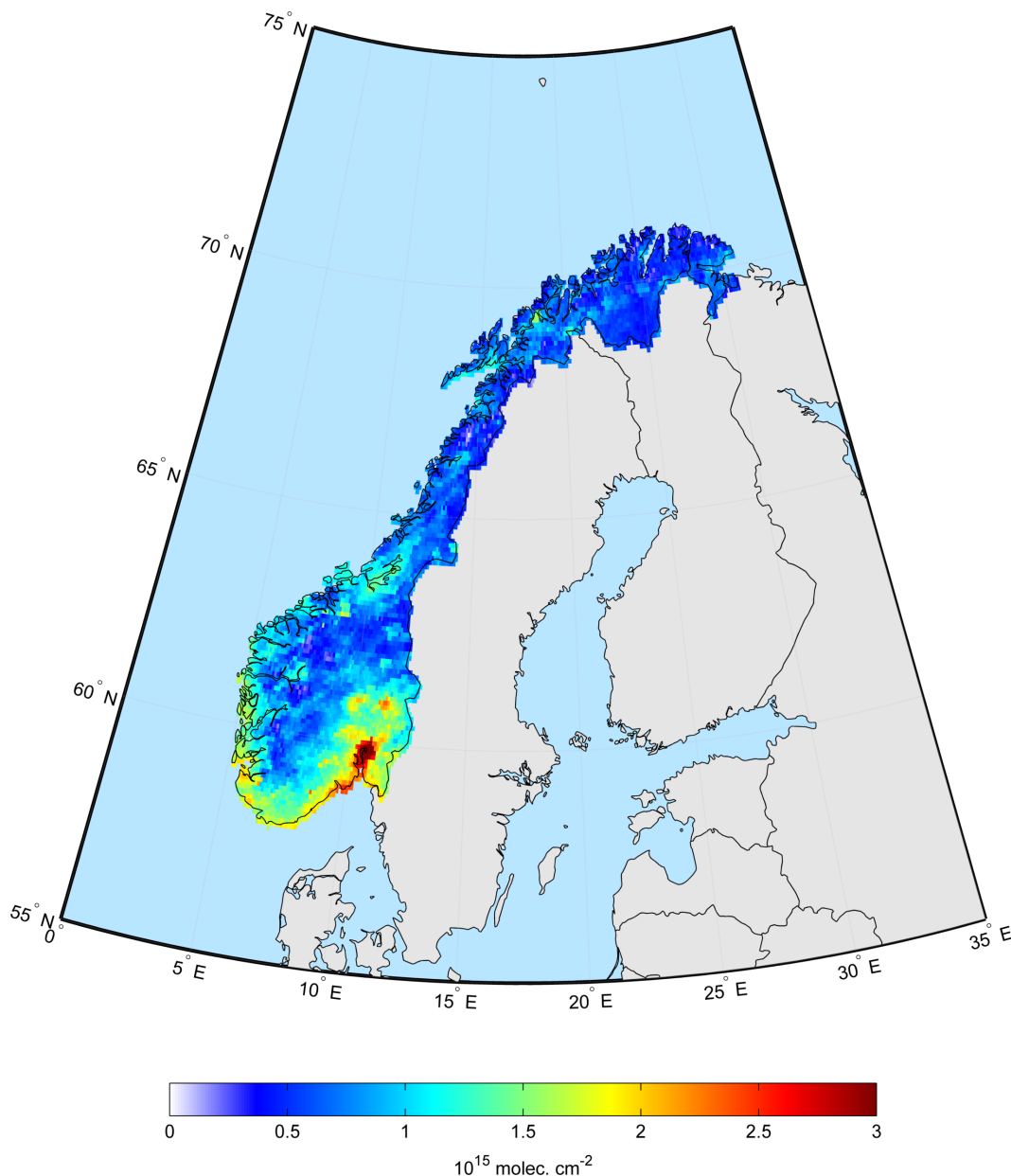


Figure 13 Annual average tropospheric NO₂ column for the year 2009 over Norway. Derived from the 0.1 degree high-resolution OMNO2e product. This figure shows the same data as displayed in Figure 11 however it uses a modified color scale in order to highlight spatial patterns of NO₂ in Norway.

4.1.2 Kriging NO₂ in Norway using Airbase and OMI satellite data

Based on the results reported on in the previous section and in order to provide an indication as to what extent satellite data of NO₂ can help to improve European-scale mapping of air quality, OMI-based tropospheric column NO₂ data was subsequently used in the next step to complement the station measurements from Airbase (see Figure 4) as an auxiliary dataset. As described in detail in the methodology section, this was accomplished by establishing a correlation between the station-based NO₂ means and the mean satellite-based tropospheric columns as observed over each station.

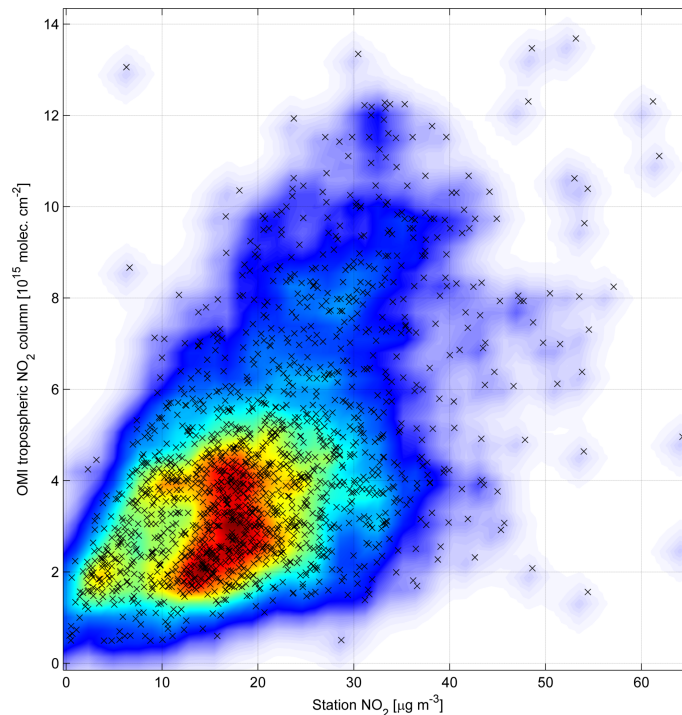


Figure 14 Scatterplot of Airbase-derived annual mean 2009 station NO_2 concentration against the 2009 annual mean tropospheric NO_2 columns derived from the OMNO2e high-resolution product.

Figure 13 shows the 2009 average tropospheric NO_2 column over Norway based on the OMNO2e $0.1^\circ \times 0.1^\circ$ resolution satellite product. This map is similar to the one shown in Figure 11 but it has a modified color scale in order to better highlight the spatial patterns within the overall low values of the tropospheric NO_2 column in Norway.

Figure 14 shows a scatter plot indicating the correlation between the 2009 annual average NO_2 concentration at all background Airbase stations and the 2009 annual average tropospheric column extracted at each station location from the high-resolution annual average OMI dataset. A linear model was fitted to this dataset as

$$C_{OMI} = 1.89 + 0.12 \times C_{St} \quad (6)$$

where C_{OMI} is the tropospheric column observed by the OMI instrument and C_{St} is the annual mean NO_2 concentration observed at each Airbase station. The R^2 value of the model was found to be close to 0.3.

At first glance this correlation might appear to be quite weak, however it needs to be considered that this analysis compares two parameters which have very different spatial and temporal scales. While the station observations provide an annual mean NO_2 value at the ground level computed from hourly values and which is representative of only a very small area, the satellite instrument provides the total number of NO_2 molecules at 14:00 local time, averaged not only over a 100 km^2 area but also integrated over the entire troposphere. Given these fundamental differences in spatial and temporal scales, the correlation seen in Figure 14 is quite reasonable.

The residuals resulting from the fitted linear regression are shown in Figure 16 for all of Europe. As mentioned before, while the goal of this project was to map background concentrations in Norway, the geostatistical analysis had to be performed

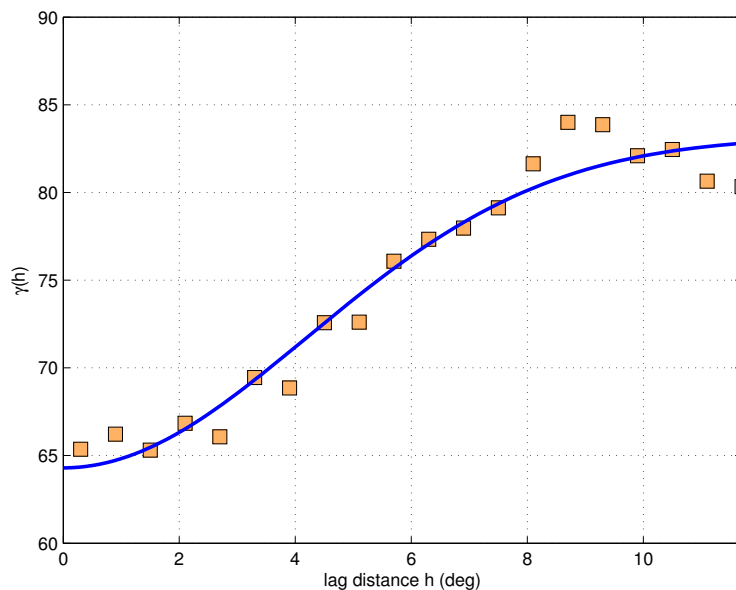


Figure 15 Empirical and modeled semivariogram of the residuals (shown in Figure 16). The model is a combination of a nugget effect of 64.3 and a Gaussian model with range 5.9 and a sill of 18.9.

at the European level in order to obtain enough sampling points for deriving a representative semivariogram model. In addition, Figure 17 shows the residuals obtained for air quality stations located in Norway only for reference.

Overall, the spatial patterns in the residuals indicate negative values throughout the northern part of Central Europe, i.e. in Germany, the Netherlands, Belgium, and the western part of Poland. Positive residuals can be found throughout most of the rest of Europe, however the highest density of positive residuals occurs in Northern Italy and the east of France. In Norway, the situation is mixed, with stations in Oslo, Kristiansand, and Bergen, and Lillehammer showing positive residuals while the rest of the stations has negative residuals. In particular the entire northern half of the country exhibits negative residuals.

The residuals were then subsequently plotted as an empirical semivariogram, which was then in turn modeled using a combined nugget effect of 64.3 and a Gaussian model with range 5.9 degrees and a sill of 18.9 (see Figure 15). The semivariogram model was then used to kriged the residuals from the previously discussed linear regression over the entire study domain. This domain ranged from 20° N to 73° N and from 20° W to 40° E. A spatial resolution of 0.1° was used for the final grid. Figure 18 shows the kriged residuals over all of Europe.

A final map of NO₂ was then generated by combining the regressed map with the map of the kriged residuals. The result of this effort is shown in Figure 19. As would be expected, the spatial patterns of NO₂ in Norway contain elements of both the OMI satellite dataset and the kriged residuals of the station observations.

When qualitatively comparing the spatial patterns found in the original map of the satellite measurements of NO₂ tropospheric column (Figure 13) with the final map of NO₂ found in Figure 19, it can be observed that the southwestern part of the country now has slightly higher values than before due to the impact of the positive residuals (which were primarily caused by a strong positive value at the Bergen station).

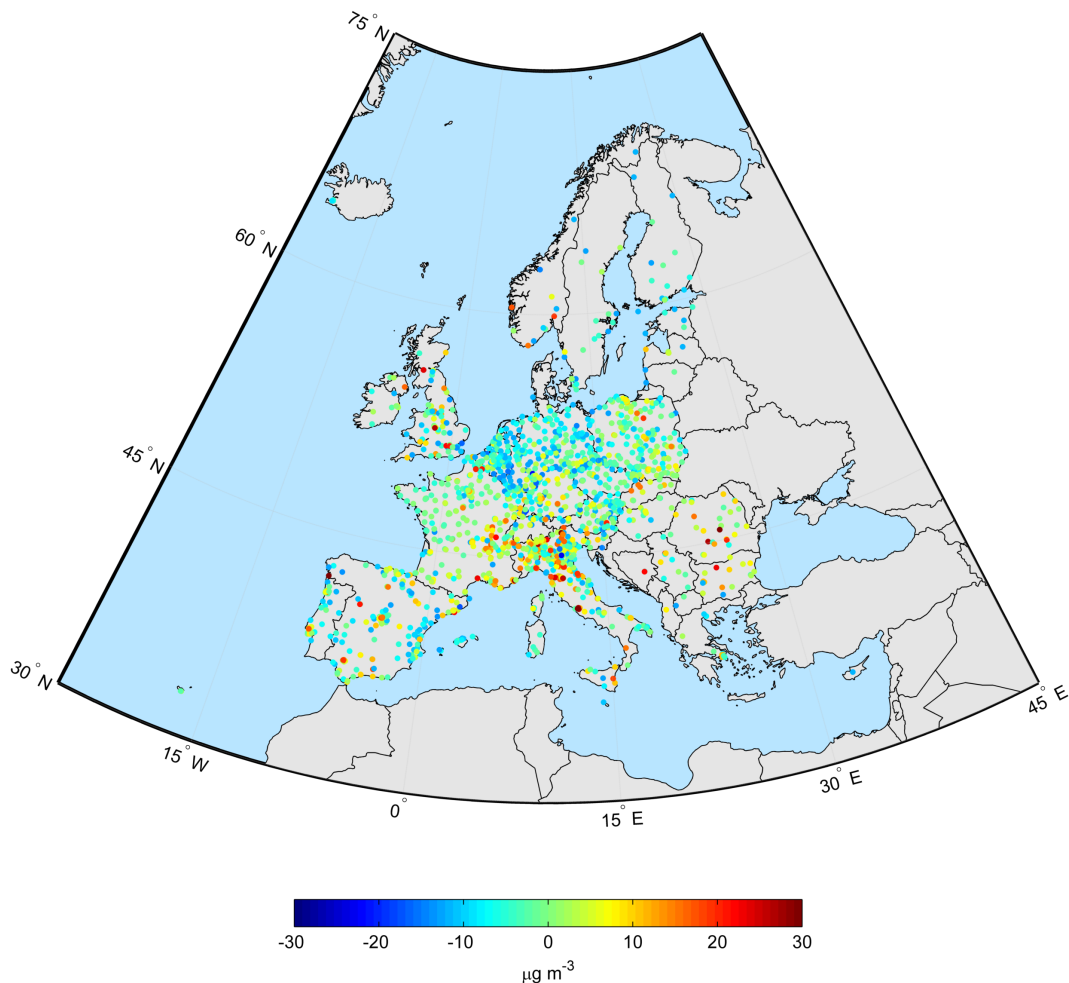


Figure 16 Map showing the residuals from the model fitted between the average 2009 NO₂ at all Airbase background stations and the mean tropospheric NO₂ column provided by the high-resolution OMNO2e product.

A very preliminary validation of the data was carried out at the European level. Cross-validation was used to evaluate the quality of the results. Based on this validation technique, the original Airbase dataset was randomly split up in two parts. The first part, encompassing 90% of the stations, was used within the kriging procedure. The second part, consisting of approximately 10% of the Airbase stations was used solely for validation purposes. This procedure ensures that the stations used for validation had absolutely no impact on the quality of the result as they were not used as part of the algorithm. This resulted in a total number of 198 randomly selected stations that were separated from the main Airbase dataset and only used for validation purposes. The validation for this map resulted in an RMSE of $8.5 \mu\text{g m}^{-3}$ at the European level, which is lower than the mapping carried out using solely station data (RMSE = $9.1 \mu\text{g m}^{-3}$). As expected, this indicates that the satellite dataset provides additional valuable information on spatial patterns.

The results of this part of the study indicate that satellite data can be very useful as an auxiliary variable in mapping air quality at both the European and Norwegian scale. Using tropospheric column NO₂ data acquired by the OMI instrument provided significantly better mapping results (both qualitatively as well as quantitatively) than geostatistical interpolation of station data alone.

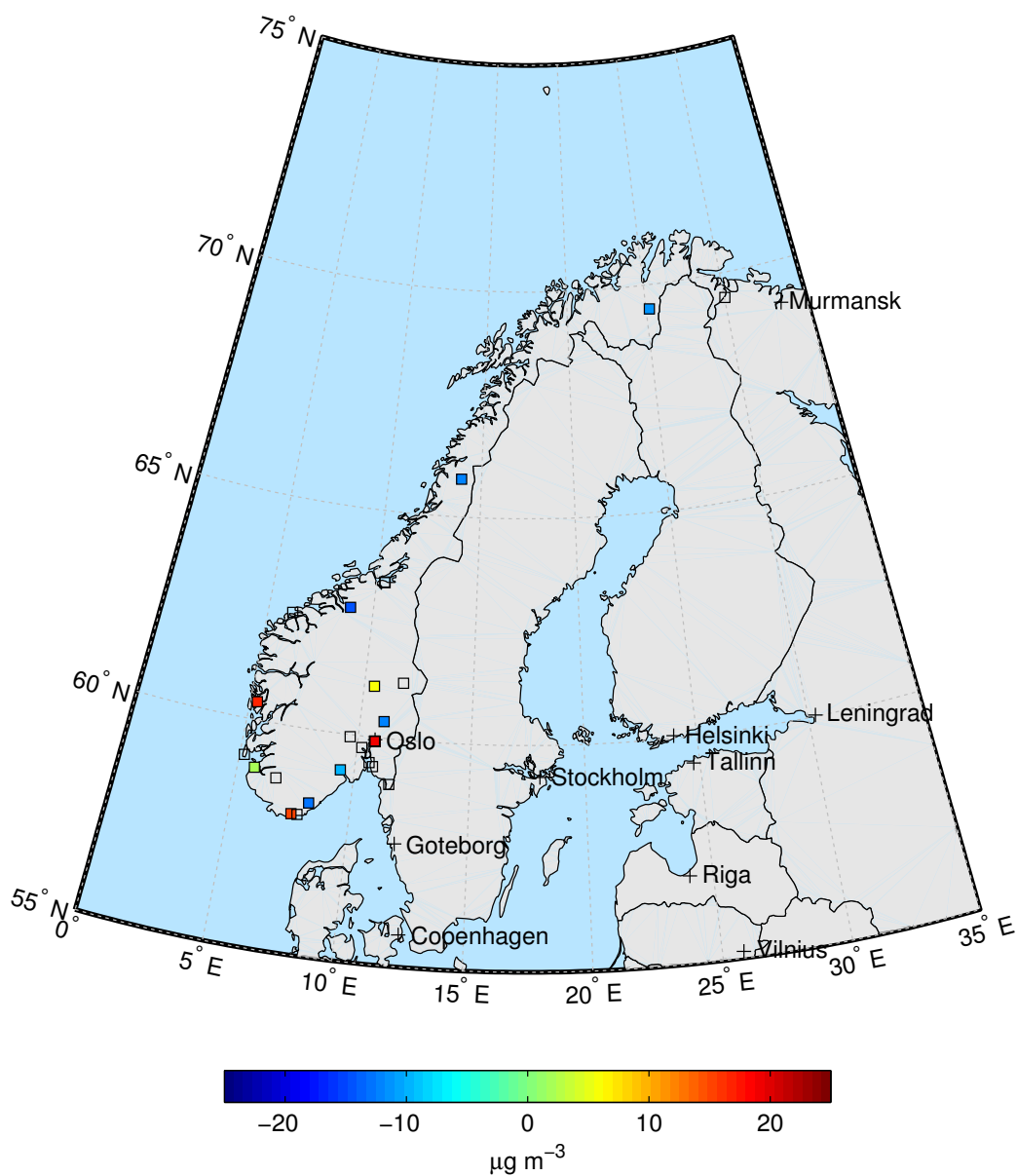


Figure 17 Map showing the residuals from the model fitted between the average 2009 NO₂ at all Airbase background stations in Norway and the mean tropospheric NO₂ column provided by the high-resolution OMNO2e product. Please refer to Figure 5 as a reference for identifying the individual stations.

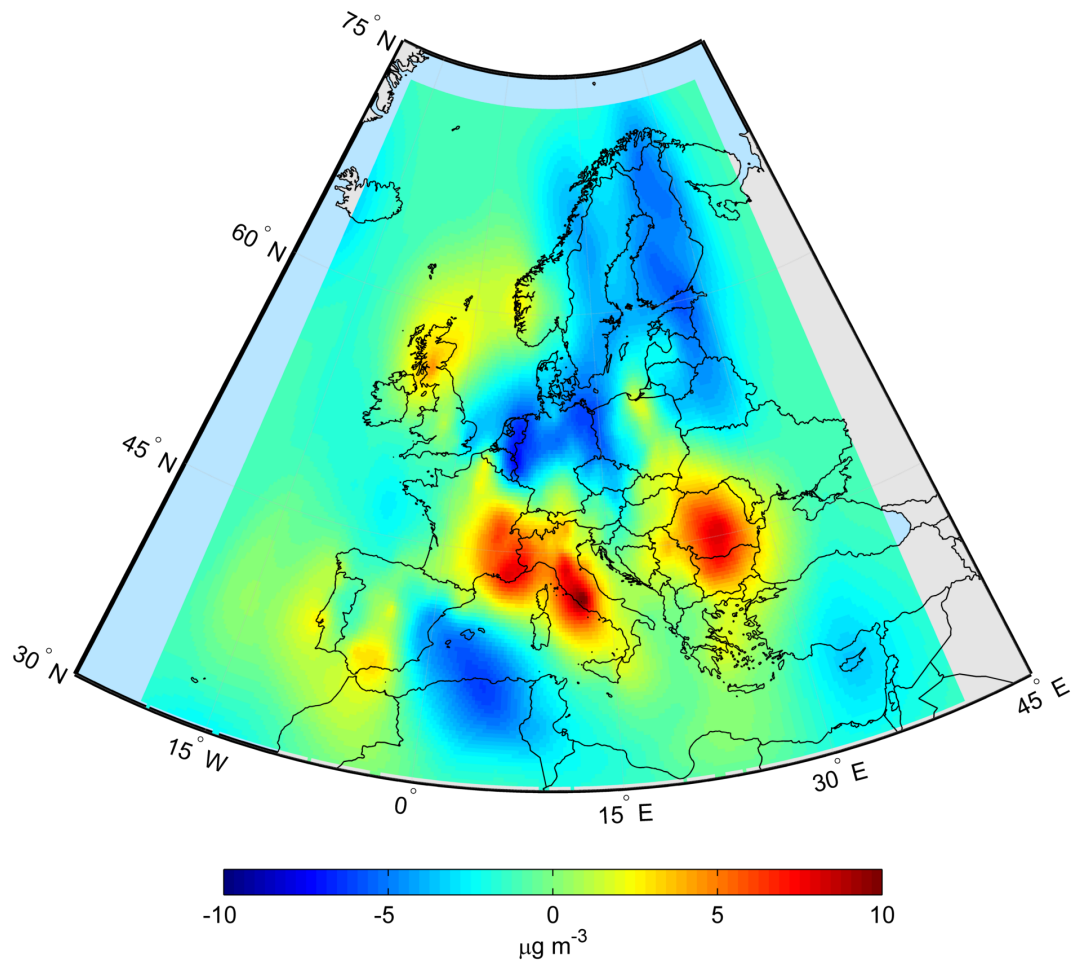


Figure 18 Map showing the geostatistically interpolated residuals given at the station level in Figure 16. The interpolation was carried out by kriging using the semivariogram model indicated in Figure 15. The grid size used was $0.1^\circ \times 0.1^\circ$.

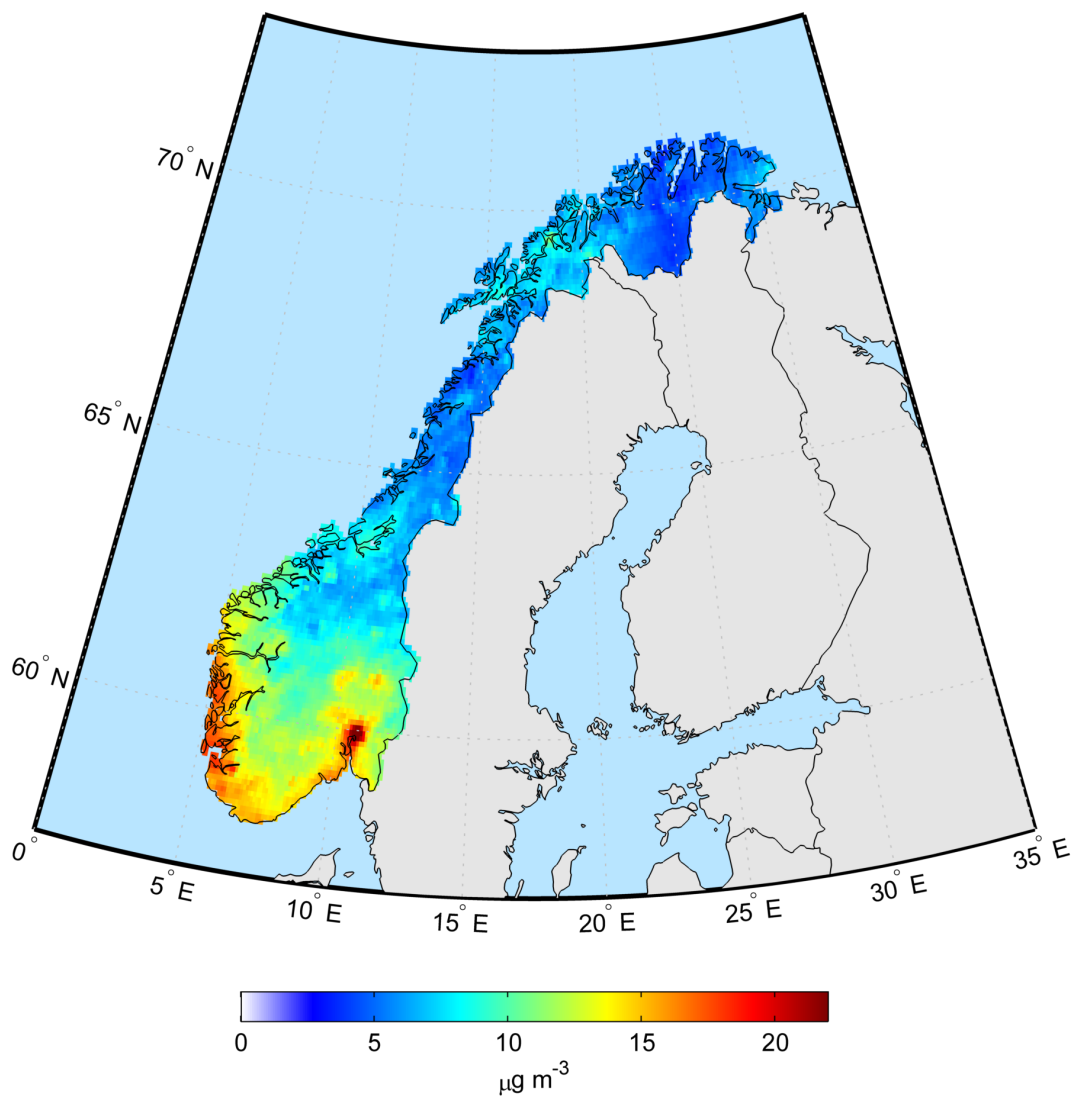


Figure 19 The average NO₂ concentration in Norway for 2009. The data is based on the residual kriging of Airbase station data and using OMI satellite data (more specifically the experimental OMNO2e 0.1° × 0.1° resolution product) as an auxiliary dataset.

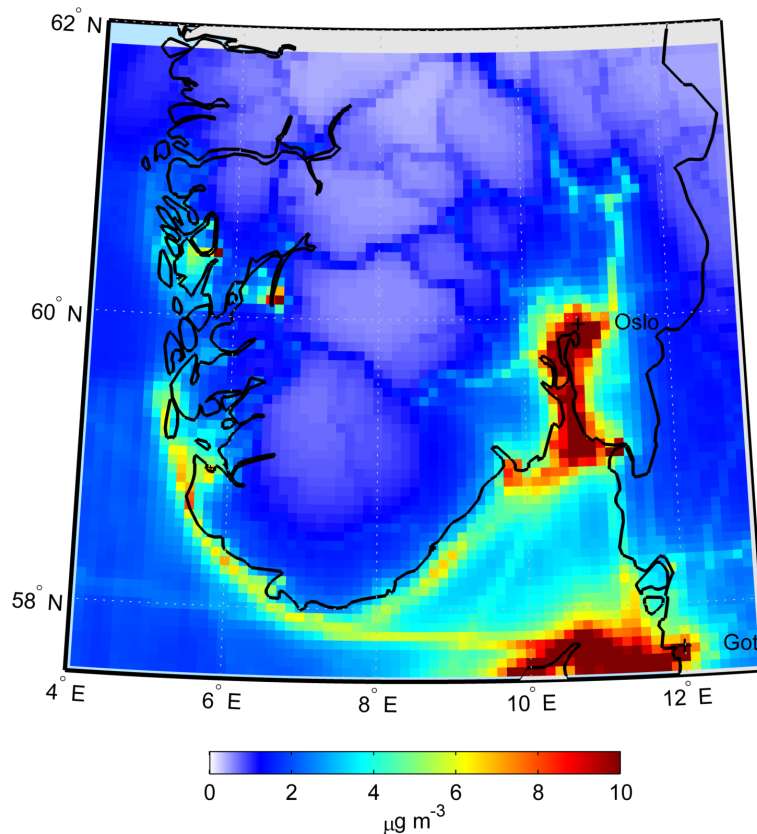


Figure 20 Annual mean NO₂ concentration over southern Norway as computed by the CHIMERE chemical transport model.

4.2 Using high-resolution model output

While station observations can provide highly accurate information on air quality, obtaining detailed spatially distributed estimates generally requires the use of some kind of auxiliary data set. In the previous section, the usefulness of satellite data for purposes of NO₂ mapping was evaluated. Here, high-resolution output from the atmospheric chemistry transport model CHIMERE (Schmidt et al., 2001; Vautard et al., 2001; Bessagnet et al., 2004) is evaluated with respect to its suitability of contributing both spatial and temporal information to the estimation process.

In order to get an idea about the spatial patterns produced by the CHIMERE model, in a first step an annual average NO₂ concentration was computed from the hourly values. The result is shown in Figure 20, giving the 2009 average NO₂ concentration over southern Norway as provided by the CHIMERE chemical transport model. A large area of high average NO₂ concentrations (exceeding 10 μg m⁻³) is visible all along the Oslo Fjord. A few other grid cells near Stavanger, Bergen, and Odda also exceed this value, however most of the rest of the land areas exhibits very low average NO₂ concentrations below 2 μg m⁻³. Major transportation routes are clearly visible as linear features of small mean annual concentration between 1 μg m⁻³ and 2 μg m⁻³ while the NO₂ concentration in the surrounding areas is essentially zero. Along the entire coast line of southern Norway emissions from shipping traffic cause annual average NO₂ concentrations around 6 μg m⁻³.

In a next step, time series produced by the CHIMERE model were evaluated and the degree of correlation between station observations and the corresponding CHIMERE

Table 3 Result of simple linear regression between the 2009 hourly time series of NO₂ from station measurements in southern Norway and the corresponding time series extracted from the CHIMERE output over the same locations.

Station	Intercept	Slope	R ²
Rådhuset	3.72	0.19	0.22
Haukenes	4.00	0.26	0.11
Stener Heyerdahl	7.51	-0.02	0.00
Våland	5.92	0.36	0.20
Lillehammer Barnehaugen	2.82	0.16	0.16
Øyekast	5.87	0.12	0.07

time series was quantified. This was accomplished by plotting the time series of the two datasets for each station and each of the four species (NO₂, O₃, PM₁₀, PM_{2.5}), followed by the corresponding scatterplot visualizing the correlation between the two datasets. This was then further quantified by fitting a linear regression model to the two datasets and calculating the regression statistics. In the following paragraphs, the results are summarized for each of the four species.

4.2.1 NO₂

Figure 21 shows a comparison of hourly observations of NO₂ at several air quality stations in southern Norway with the output from the high-resolution CHIMERE model run extracted over the same locations. It is clear from the figure that while the model is able to capture some of the temporal variability and the related patterns, the absolute values deviate substantially from the observations.

In order to visualize the correlation between the modeled time series and observed time series at the stations, Figure 22 shows scatter plots between the two variables (given here technically as 2-dimensional density plots). As supplemental information the regression statistics of a linear model fitted to the relationships shown in Figure 22 is given in Table 3.

The strongest correlation with an R² value of 0.22 is found at the Rådhuset station, however the slope value of 0.19 as well as a visual interpretation of the corresponding scatterplot indicate that the model significantly underestimates the absolute values at this location. A similar correlation between the two variables is found at the Våland station which has an R² of 0.20 and a slope of about 0.36, indicating also here a significant underestimation of the actual observed surface NO₂ concentrations. The linear regression models at all other stations either exhibit very low R² values or a very low slope value and thus showing even more significant biases.

4.2.2 O₃

Figure 23 shows the hourly time series of O₃ in 2009 for both the station observations at 7 stations located in southern Norway and the corresponding time series of surface O₃ predicted by the CHIMERE chemical transport model at the same locations. The two time series appear to agree quite well at the various stations, in particular during the first half of the year. While obviously short-term temporal variability cannot be

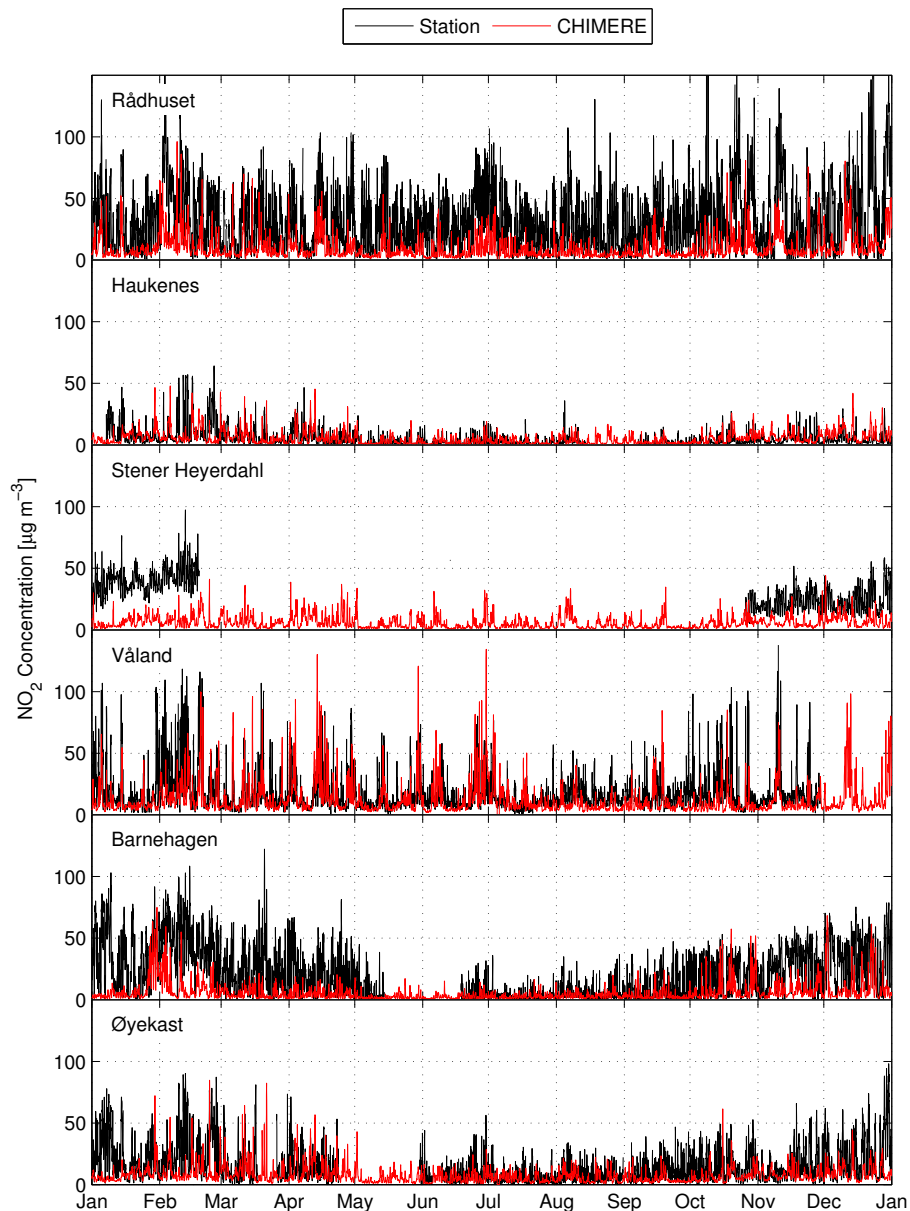


Figure 21 Comparison of 2009 hourly time series of NO_2 from station measurements in southern Norway and the corresponding time series extracted from the CHIMERE output over the same locations.

replicated by the model, the longer-term changes are generally well captured. During the second half of the year the CHIMERE results generally overestimate the true value given by the observations.

A visual representation of the correlation between the station observations and the model results can be found in Figure 24. The results corroborate the first impression from Figure 23 in that the correlation between the observations and the model data for O_3 appear to be much stronger than previously found for NO_2 . In particular the stations Prestebakke and Hurdal indicate a very good correlation.

This is further shown in Table 4 which indicates R^2 values of 0.57 and 0.50 for Prestebakke and Hurdal, respectively. The statistics of the linear regression model at the other stations all exhibit R^2 values of greater than 0.35, which is more than the

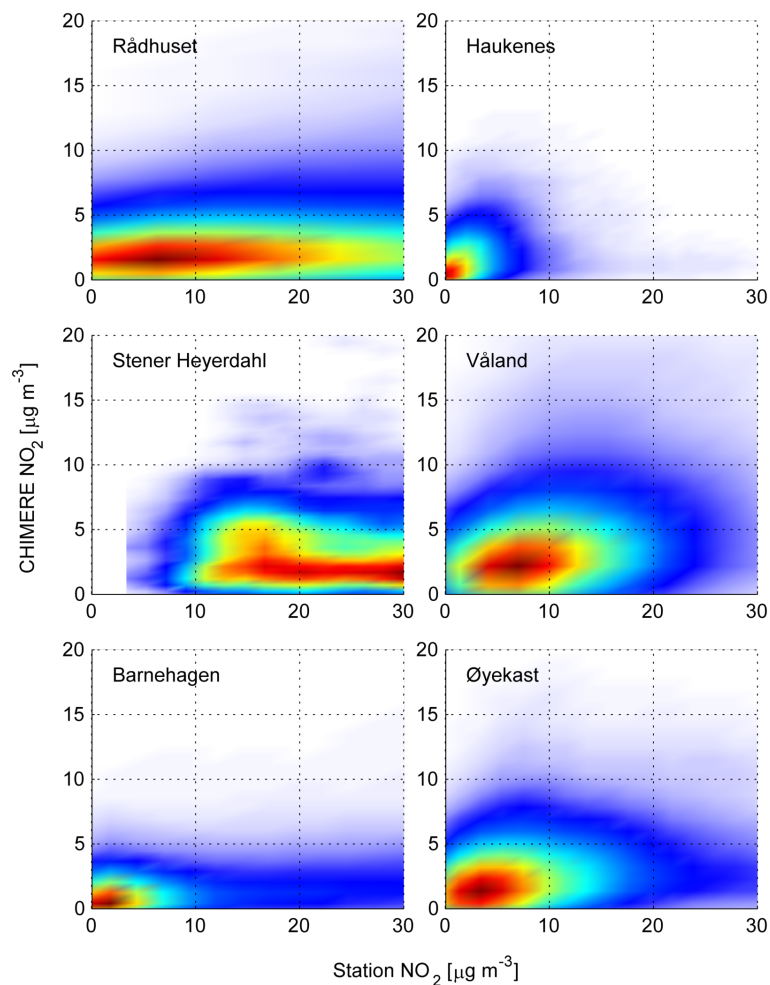


Figure 22 Comparison of 2009 hourly time series of NO_2 from station measurements in southern Norway and the corresponding time series extracted from the CHIMERE output over the same locations, here shown as a two-dimensional histograms (or density plots).

CHIMERE model achieved at any of the stations at which NO_2 was measured (see Table 3).

4.2.3 PM_{10}

Figure 25 shows the hourly time series of PM_{10} in 2009 for both the station observations at 7 stations located in southern Norway and the corresponding time series of surface PM_{10} predicted by the CHIMERE chemical transport model at the same locations. It is obvious at first glance that the model is not capable of reproducing the extremely high temporal variability of the PM_{10} concentrations as they are measured at the various stations. The time series of the model for the most part follows the minimum observed concentrations and can to some extent actually trace some of the longer-term patterns in the minimum values. However, given that hourly values are compared here and that the temporal variability of PM_{10} is extremely high, the differences between the model and the station observations are quite large and exceed $100 \mu\text{g m}^{-3}$ in many instances.

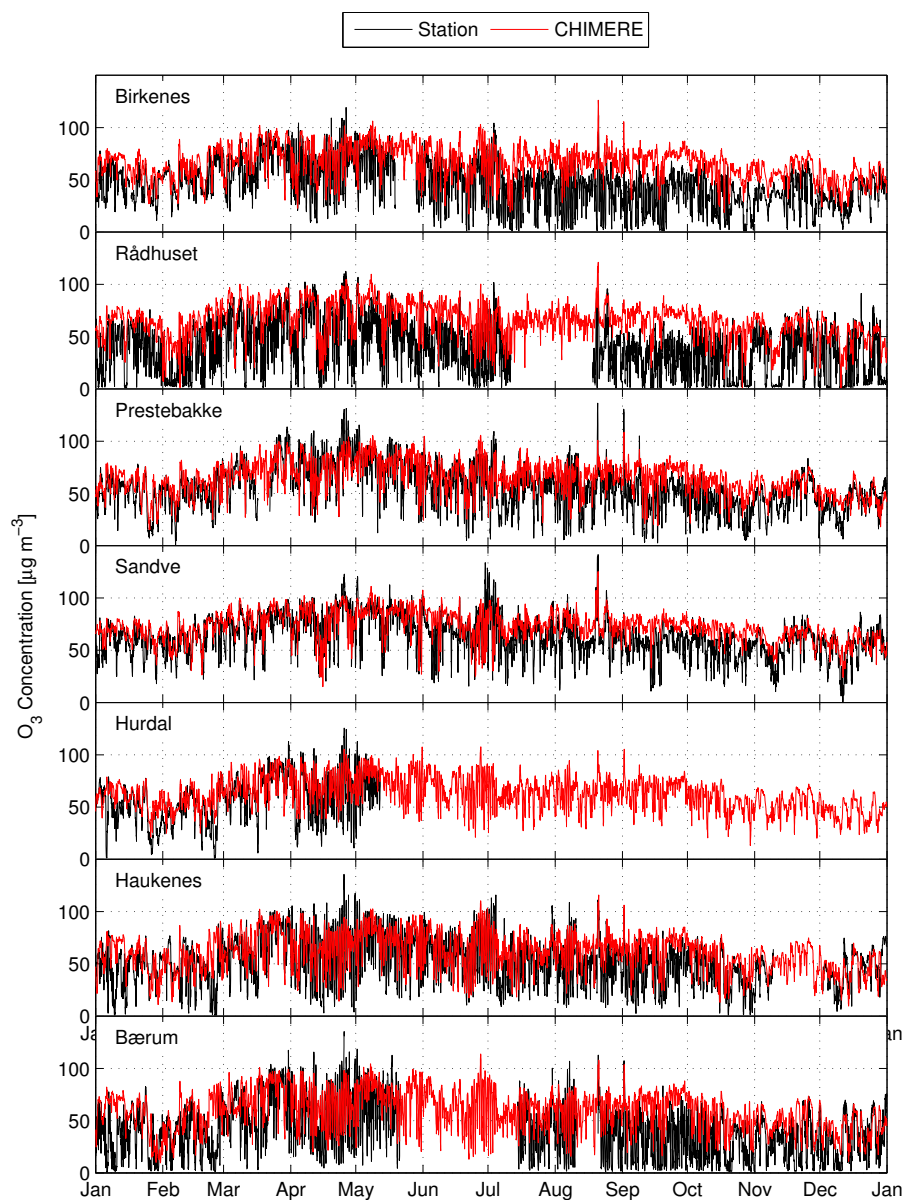


Figure 23 Comparison of 2009 hourly time series of O_3 from station measurements in southern Norway and the corresponding time series extracted from the CHIMERE output over the same locations.

Table 4 Result of simple linear regression between the 2009 hourly time series of O_3 from station measurements in southern Norway and the corresponding time series extracted from the CHIMERE output over the same locations.

Station	Intercept	Slope	R^2
Birkenes	45.32	0.44	0.39
Rådhuset	46.51	0.47	0.44
Prestebakke	34.56	0.54	0.57
Sandve	42.06	0.48	0.40
Hurdal	37.32	0.50	0.50
Haukenes	36.67	0.48	0.36
Bærum	40.21	0.45	0.37

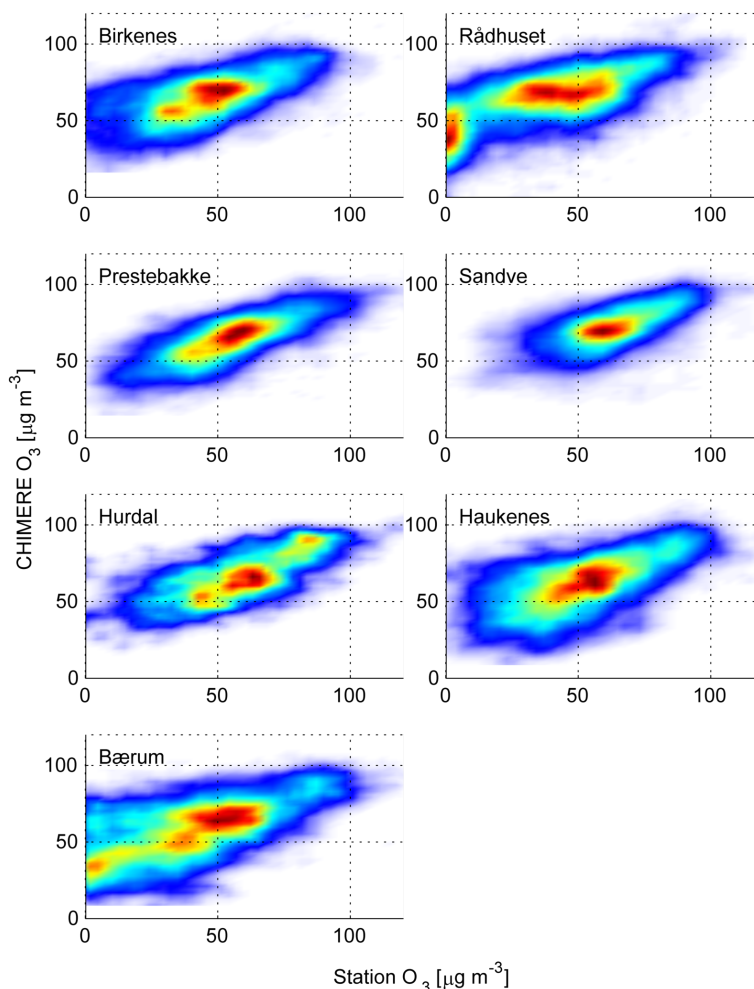


Figure 24 Comparison of 2009 hourly time series of O₃ from station measurements in southern Norway and the corresponding time series extracted from the CHIMERE output over the same locations, here shown as two-dimensional histograms (or density plots).

The lack of correlation becomes even more obvious in Figure 26, showing scatter plots between station observations and model data for all the seven stations. For most of the stations, hardly any correlation is visible, at least when considering the entire range of values. The statistics of the linear regression model for each station are given in Table 5). The R^2 values of the fitted linear models are less than 0.1 throughout all of the stations considered and thus indicate that the CHIMERE model is not able to replicate the short-term temporal variability of PM₁₀ time series in Norway.

4.2.4 PM_{2.5}

Figure 27 shows time series for station observations of PM_{2.5} and the corresponding CHIMERE model output for two stations in southern Norway at which PM_{2.5} was measured in 2009. The overall levels of PM_{2.5} appear to match quite well between the two datasets. No strong biases, as they were for example visible at some of the stations measuring NO₂, are visible for either station. However, while the modeled time series appear to trace mostly the lower range of observed values, a lot of short-term temporal variability is not adequately covered. This is particularly obvious for the Barnehaugen station where many observed short-term spikes in the data during

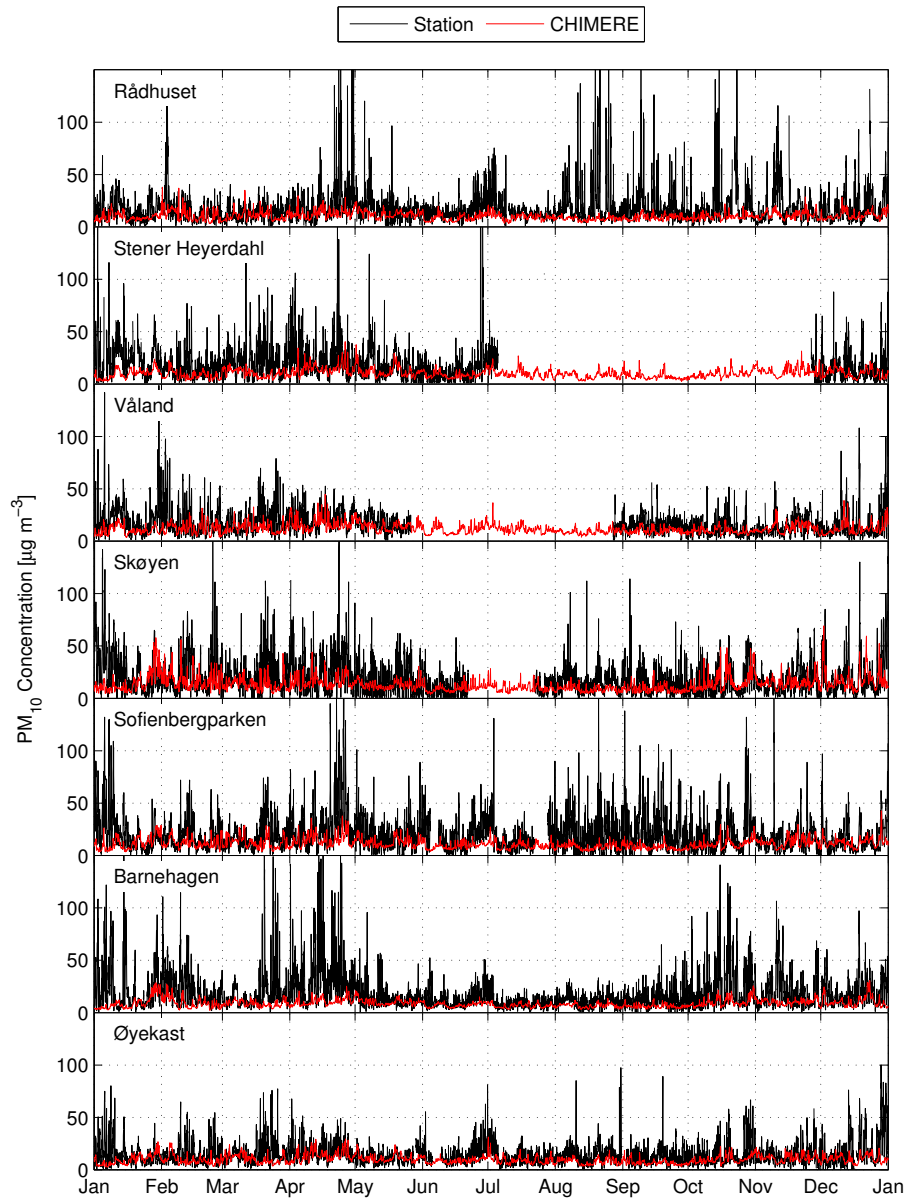


Figure 25 Comparison of 2009 hourly time series of PM_{10} from station measurements in southern Norway and the corresponding time series extracted from the CHIMERE output over the same locations.

Table 5 Result of simple linear regression between the 2009 hourly time series of PM_{10} from station measurements in southern Norway and the corresponding time series extracted from the CHIMERE output over the same locations.

Station	Intercept	Slope	R^2
Rådhuset	9.73	0.03	0.02
Stener Heyerdahl	9.85	0.04	0.02
Våland	10.29	0.11	0.09
Skøyen	11.63	0.08	0.04
Sofienbergparken	10.20	0.05	0.03
Barnehaven	7.80	0.05	0.05
Øyekast	9.01	0.05	0.02

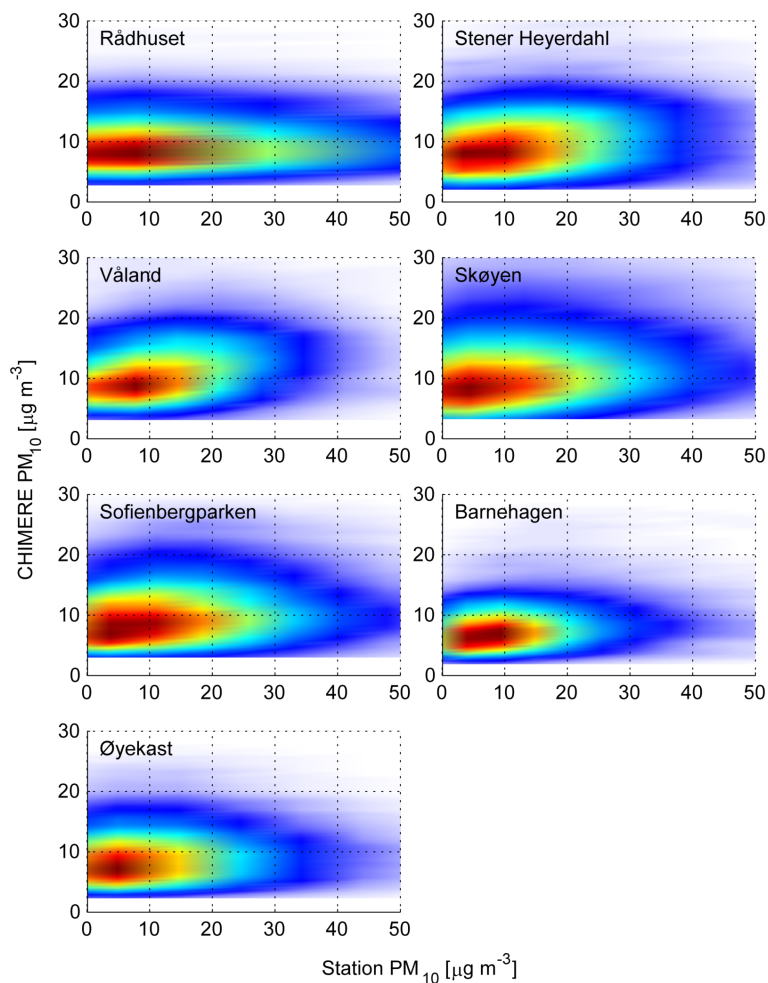


Figure 26 Comparison of 2009 hourly time series of PM_{10} from station measurements in southern Norway and the corresponding time series extracted from the CHIMERE output over the same locations, here shown as a two-dimensional histograms (or density plots).

the winter months exceed $30 \mu\text{g m}^{-3}$. Hardly any of this high-frequency temporal variability is replicated by the modeled time series. However, it should be noted that some of the slightly lower-frequency temporal variability such as the increase at the Barnehaugen station in late January and early February was able to be captured by the model. In addition, some individual spikes, for example at the Våland station in early and late December were also replicated by the model.

The situation can be observed even more clearly in the scatterplots or two-dimensional histograms, given in Figure 28. Both scatterplots indicate that the two station and model time series appear to have only a very weak correlation. Whereas hardly any correlation can be observed for the Våland station, a slight correlation appears to be visible at the Barnehaugen station for low observed values of $\text{PM}_{2.5}$ between 0 and $10 \mu\text{g m}^{-3}$.

The lack of a strong correlation between station observations of $\text{PM}_{2.5}$ and the corresponding CHIMERE model results is quantified in the statistics of the linear regression models, as indicated in Table 6. Both stations have very low R^2 values of 0.13 and 0.07 for Våland and Barnehaugen, respectively. While these are slightly higher on average than the regression results obtained for the PM_{10} time series (Table 5), it is

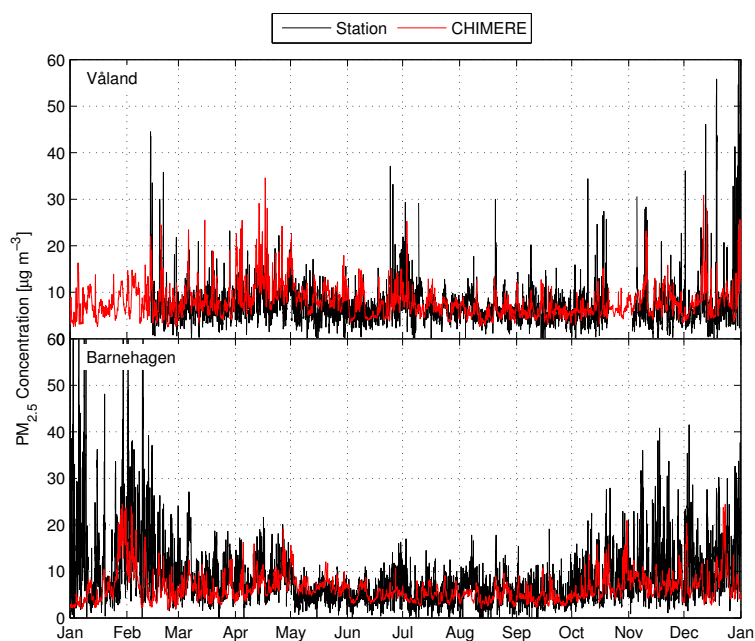


Figure 27 Comparison of 2009 hourly time series of $\text{PM}_{2.5}$ from station measurements in southern Norway and the corresponding time series extracted from the CHIMERE output over the same locations.

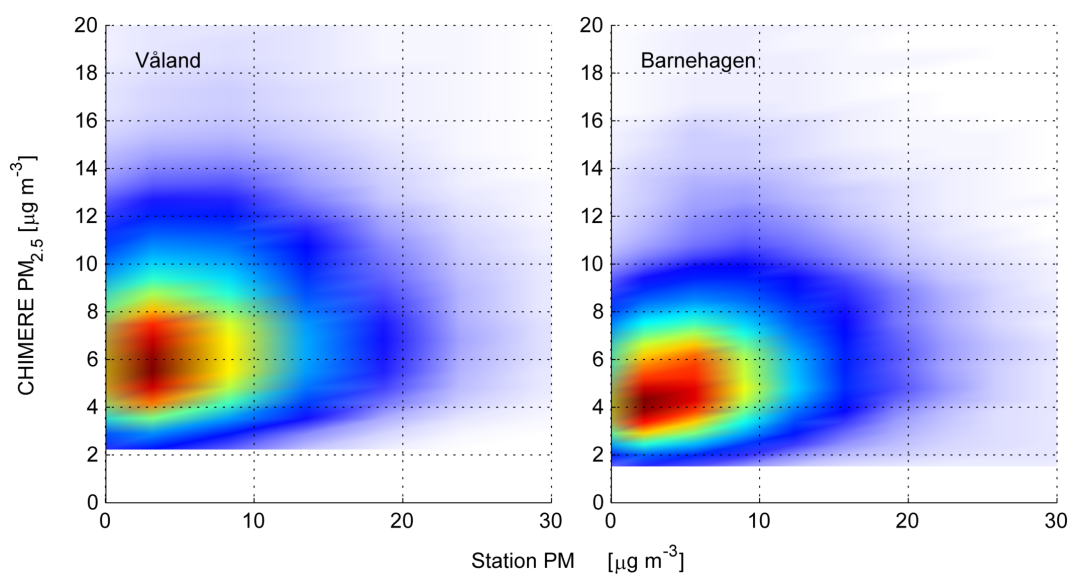


Figure 28 Comparison of 2009 hourly time series of $\text{PM}_{2.5}$ from station measurements in southern Norway and the corresponding time series extracted from the CHIMERE output over the same locations, here shown as two-dimensional histograms (or density plots).

Table 6 Result of simple linear regression between the 2009 hourly time series of $\text{PM}_{2.5}$ from station measurements in southern Norway and the corresponding time series extracted from the CHIMERE output over the same locations.

Station	Intercept	Slope	R^2
Vålånd	6.41	0.20	0.13
Barnehaugen	5.24	0.13	0.07

still too low to use the CHIMERE model time series as a direct substitute for hourly station observations when high frequency temporal variability is of particular interest.

4.2.5 Evaluation for estimation of background concentrations in Norway

Given the generally weak correlation between hourly station observations and CHIMERE model results as reported on in the previous sections, it appears as if the model output investigated here is currently not too suitable to replace station observations as a reliable information source on high-frequency temporal variability. One exception could be O₃ for which reasonably strong correlations with R² values of up to 0.6 were found. However, correlations for NO₂ and particularly PM₁₀ and PM_{2.5} were unacceptably weak. In addition to the relatively weak correlation between station observations and the model output, another issue concerning the use of model output for the temporal component of the methodology is the lack of long model-based time series at hourly resolution (see Section 1 for more information on the distinction between spatial and temporal component). Only one year of high-resolution hourly CHIMERE data was available for this project (2009). The lack of long time series of high-resolution model output is of course not surprising since running chemical transport models such as CHIMERE at not only a high spatial resolution (less than 10 km × 10 km) but at the same time at a high temporal resolution (hourly sampling or better) is extremely demanding on the required computational resources and is at this point in general not performed operationally. On the other hand, the temporal component in the standard methodology for estimating Norwegian background concentrations as described in Schneider et al. (2011) uses the average annual cycle computed over a time period between five and 10 years depending on the temporal coverage of the individual stations. This averaging over a long period is very important for deriving the temporal behavior of a “typical year” as it eliminates the high-frequency variability that varies from year to year but conserves the low-frequency signal expressed as longer-term temporal patterns that occur in similar fashion each year. As such, using the anomaly approach based on long-term station averages as described in Schneider et al. (2011) is only possible when multi-year time series are available. Finally, in order to use the high-resolution CHIMERE model output for purposes of temporal characterization in an operational fashion, model data for all of Norway would be needed and not just the southern fraction of Norway as is currently the case. Again, as mentioned previously, high-resolution model runs are extremely computationally expensive and as such the model domain is generally limited to the regions of highest interest. Unfortunately, in the case of the CHIMERE model, central and northern Norway was not part of the model domain. However, other regional chemical transport models such as the Unified EMEP model (Simpson et al., 2003) do include all of Scandinavia and could be used in future work.

Given these various reasons, the one year high-resolution dataset available from CHIMERE is therefore not suitable to replace the station data for characterizing the temporal variability. However, the foreseeable future will bring tremendous increases in computing power and thus will allow for multi-year time series and a spatial expansion of the model domain. Further methodological improvements to the model might also improve the correlations between the hourly station observations and the modeled time series. While the CHIMERE model output currently does not appear very suitable to replace hourly station observations for the temporal component of the background mapping methodology, the data might very well be used as additional information within the spatial component. The European-scale mapping methodology

currently used operationally by the ETC/ACM (Horálek et al., 2007, 2010; Denby et al., 2011) already uses the output of the EMEP chemical transport model as an auxiliary variable in the residual kriging framework. Model output with significantly finer spatial resolution as the one used for this project can improve the spatial interpolation results even though the model's predictive capabilities for high-frequency temporal variability are not sufficient.

4.3 Data accessibility provided by a web mapping system

While it is crucial to evaluate potential improvements to the methodology as has been demonstrated in previous sections, providing the user easy access to the results and to visualization tools is equally important. For this reason, a web mapping system was developed at NILU in order to visualize the results of the project and to provide direct access to the data. The mapping system is a web application developed using the ASP.NET framework. It was written as a module for Sitefinity which is a web content management system provided by Telerik. The main components of the module are Microsoft Chart, jQuery UI calendar and the map displayed via GeoServer, a Java-based open-source server software designed to publish any spatial dataset using open standards. GeoServer is a reference implementation of the Open Geospatial Consortium (OGC) Web Feature Service (WFS) and Web Coverage Service (WCS) standards, as well as a high performance certified compliant Web Map Service (WMS).

Figure 29 shows a screen shot of the web mapping application that was developed as part of the project. On the upper left hand side the user can select the component of the interest (NO_2 , O_3 , PM_{10} , and $\text{PM}_{2.5}$ are available). After the map of annual average concentration is displayed in the mapping window on the right the user can freely pan the map and zoom into specific areas of interest. The data layer has been made transparent in order to allow the background map to provide reference information on location. Below the map window, a color scale indicates the concentration values that are represented by the various colors.

In addition to maps of average annual concentrations, the application further offers the possibility to visualize and extract time series at any given location within Norway. In order to do this, the user can simply click anywhere in the map and the hourly time series at the bottom of the screen (see Figure 29 bottom) will update to that particular location. Furthermore the user can also enter the exact latitude/longitude pair for any particular point of interest on the left side of the user interface and the time series figure will be updated as well. While the time series shows an entire year by default, it is also possible to specify a shorter time frame such as just a month or only a few weeks in order to see some of the temporal variability in more detail. Figures 30 and 31 show examples of the background map application for other components, areas and time periods.

The time series is the long-term average computed over the last 5 to 10 years (depending on location and data availability at the closest station) and as such represents a "typical" year. It is therefore important not to interpret the values in the time series as actual measurements or predictions but as an indication of typical magnitudes of background concentration during the last decade and their variability.

If there is an interest in using the time series data in other applications or for other purposes, it is possible to download the data of the time series by clicking the "Download Data" button. This will initiate the transfer of an ASCII file formatted using

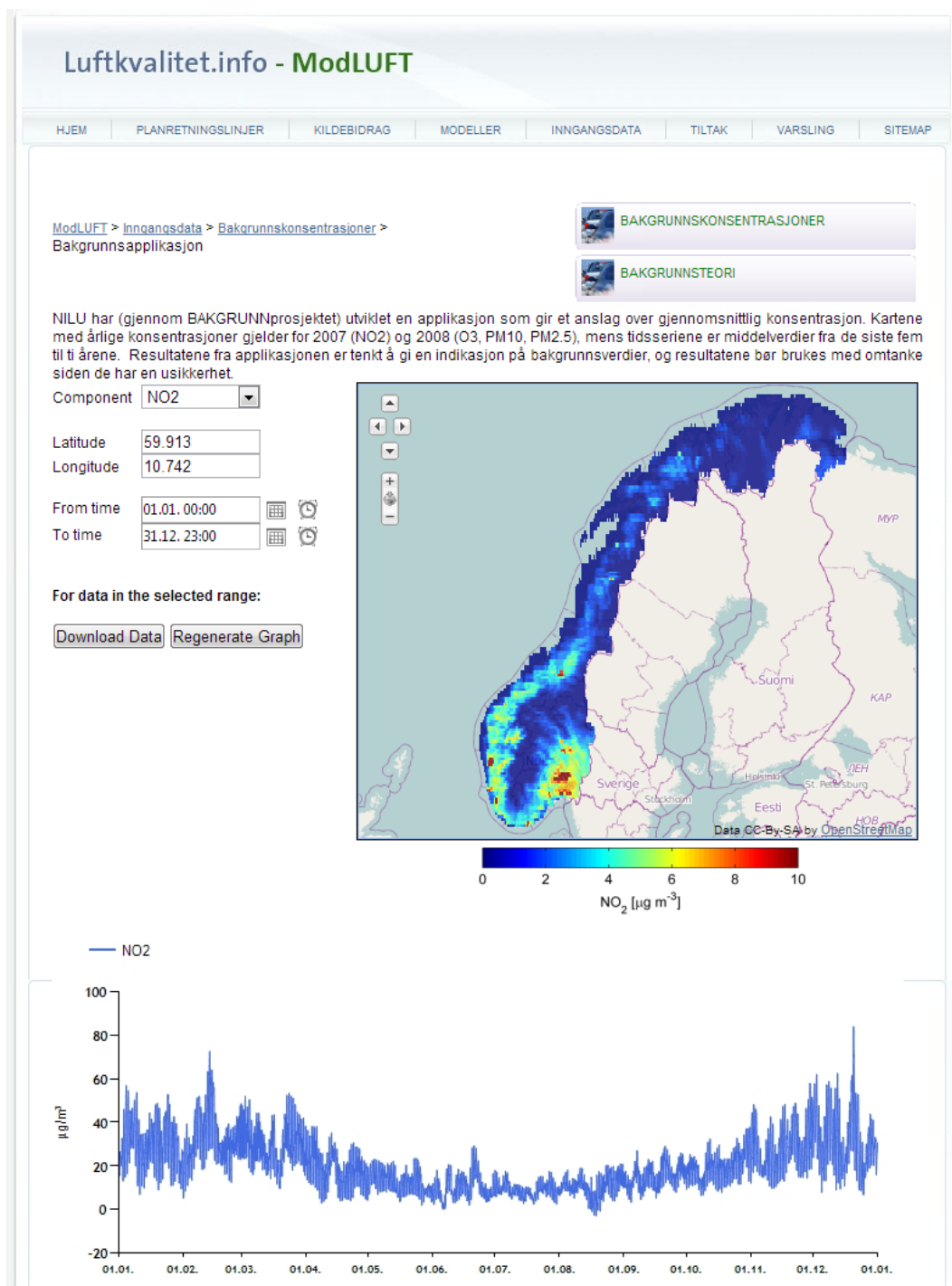


Figure 29 Screenshot of the mapping component of the online web mapping application used for visualizing the results and providing access to the data, here showing background concentrations of NO₂ throughout all of Norway and the corresponding time series for central Oslo

semicolons as a separator. The user can then further process or visualize the dataset using a program of their own choice. An example illustrating the data format is shown in Figure 32.

The web mapping application for visualizing the Norwegian background concentrations has been designed as a part of the ModLUFT web portal, which is the Norwegian National Information Center for the modeling of air quality. The web mapping applica-

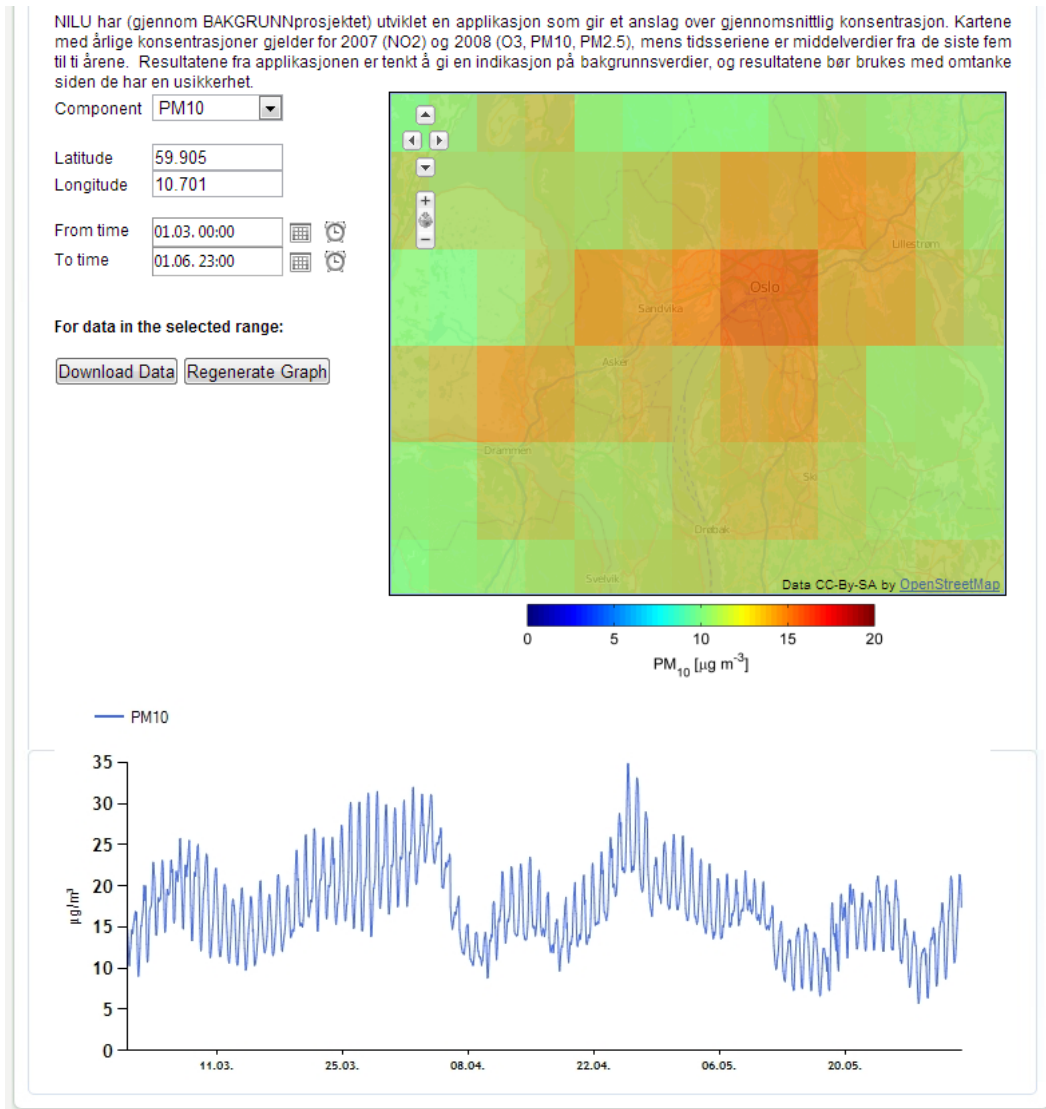


Figure 30 As Figure 29, here showing background concentrations of PM₁₀ in the greater Oslo area and the corresponding time series during the spring months. The daily variability is clearly visible from the hourly data.

tion for background concentrations is listed as part of the input datasets and has been made available at the address <http://www.luftkvalitet.info/ModLuft/Inngangsdata/Bakgrunnskonsentrasjoner/BAKGRUNNproj.aspx>.

It should be noted that both the spatial component and in particular the temporal component of the web mapping system and its underlying datasets are associated with significant uncertainties. No comprehensive validation has been performed with respect to the final values obtained from either the geostatistical mapping and the temporal analysis. While the background map data obtained from ETC/ACM has been extensively validated, the values given for individual hours of the year as provided by the dataset are associated with significant uncertainties due to several simplifying assumptions and a variety of error sources in the applied methodology. It is thus recommended to always double-check the results for potentially erroneous outliers and ideally to get advice from experts who might be able to judge the realism of the results and can provide warnings about potentially problematic predictions.

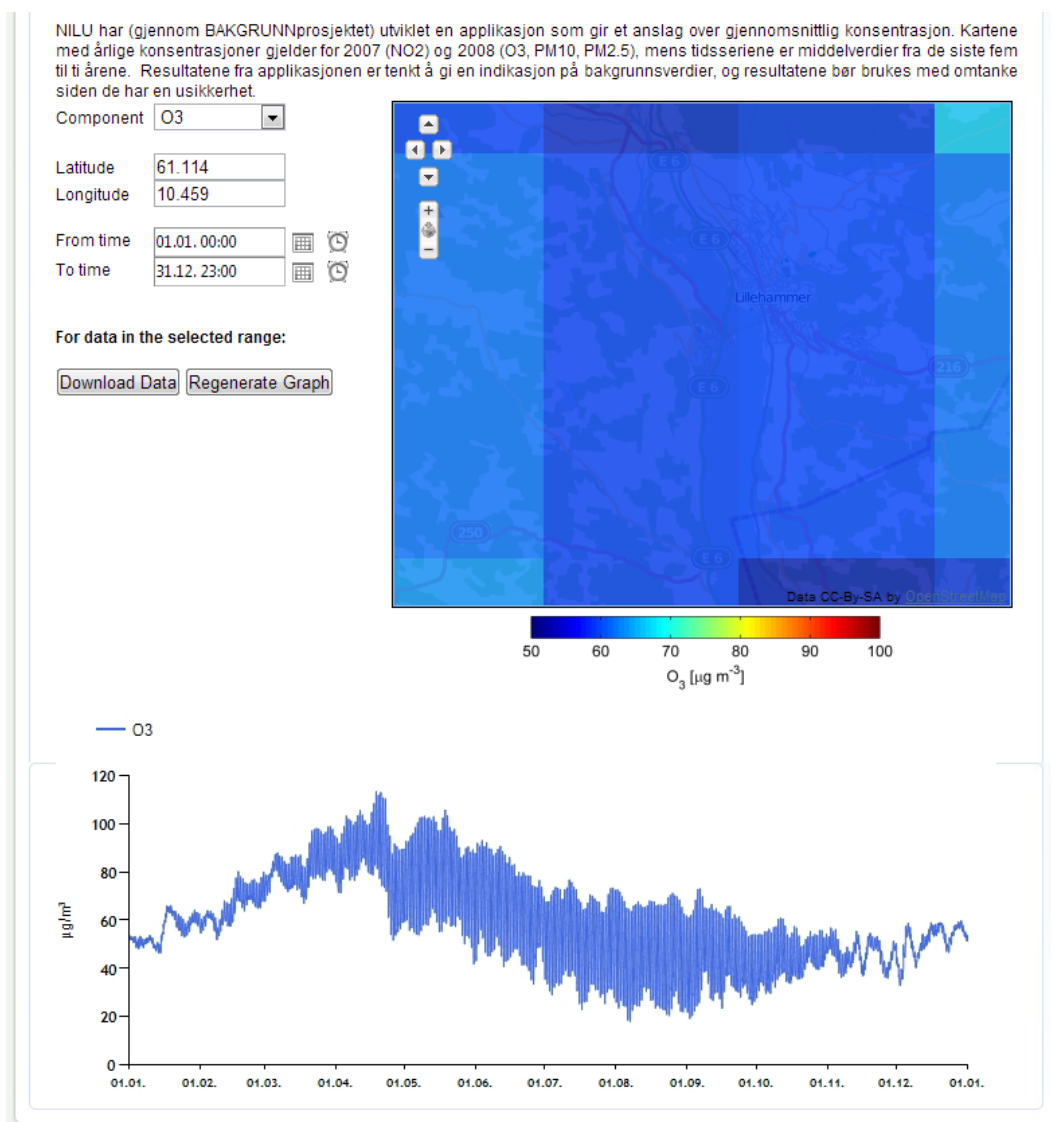


Figure 31 As Figure 29, here showing background concentrations of O₃ in the Lillehammer area.

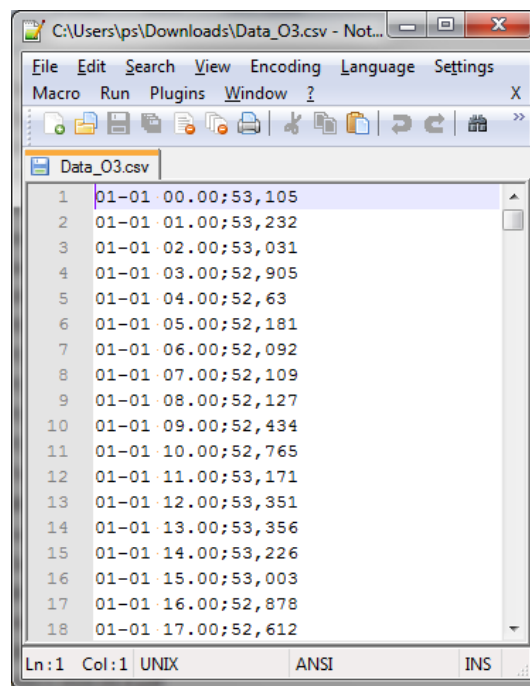


Figure 32 The actual hourly time series data for any location is provided in the form of a semicolon-separated values ASCII file after clicking the “Download Data” button in the web mapping application.

5 Conclusions

The goal of the first task of this project was to evaluate the potential of satellite data for mapping air quality, and in particular the concentrations of NO₂, in Norway. As such, a suitable NO₂ satellite product was first selected. The choice fell on a currently experimental high-resolution version of the standard OMNOe2 product produced by NASA from the OMI instrument. A statistical relationship was established between an annual average tropospheric NO₂ column dataset derived from this product and annual average NO₂ concentrations derived from Airbase station data. The obtained linear regression model was then subsequently used as an auxiliary dataset in combination with kriging of resulting residuals to generate a map of average NO₂ concentration in Norway. The results indicate that high-resolution OMI satellite data of tropospheric NO₂ columns can be very helpful as an auxiliary variable in mapping air quality. Using the additional spatially distributed NO₂ data from the OMI instrument provided significantly better mapping results than geostatistical interpolation of station data alone (as measured using the root mean squared error in a cross-validation exercise).

As a second major task, the project investigated the usability of high-resolution output from the CHIMERE chemical transport model to improve the mapping procedure. The evaluation was carried out for the four species NO₂, O₃, PM₁₀, and PM_{2.5} and consisted of a direct comparison of time series observed in 2009 at several air quality stations in southern Norway with hourly time series derived from the CHIMERE model at the exact same locations. Direct comparisons of the time series were complemented by various scatterplots and linear regression models were fitted to the resulting relationships. The results indicate that at the level of hourly temporal sampling the model is generally not able to well replicate the high-frequency temporal variability. This shows in overall very weak correlations with R² values in the range of 0 to 0.2. One exception is O₃, for which generally stronger relationships with R² values of 0.4 to 0.6 were found. These results in combination with the fact that only one year of high-resolution hourly model data was available and only the very southern part of Norway was covered by the model domain hindered the operational use of this data for supporting the temporal component of the background mapping procedure. However, the spatial component can still benefit from the high-resolution model data when using a similar residual kriging approach as used for integrating the satellite data. In addition, rapidly increasing computational power will mostly eliminate these issues in the near future. While the available dataset from the CHIMERE model unfortunately did not cover all of Norway and the developed methodology could thus not be integrated in the temporal component of the operational mapping procedure, access to other datasets will be able to change this in future. For example, the Unified EMEP (European Monitoring and Evaluation Programme, (Fagerli et al., 2011)) model (Simpson et al., 2003) has been run at a 10 km spatial resolution and its domain includes all of Norway. Unfortunately, this dataset could not be made available for the purposes of this study as the uncertainties in the high-resolution output are currently still too high to be used outside of a research environment (Michael Gauss, met.no, personal communication). However, improvements to the EMEP model are ongoing and it is likely that a future version will be made available for use in mapping Norwegian air quality.

As a third and final task, a web mapping application was developed in order to visualize both the spatial and temporal components of the background concentrations in Norway. Based on the open-source GeoServer software, the application is integrated

within the ModLuft web portal providing information about the National Information Center for the modeling of air quality. The tool provides freely zoom-able and pan-able maps of Norwegian background concentrations of the four species NO_2 , O_3 , PM_{10} , and $\text{PM}_{2.5}$. In addition, the user can display time series at any freely chosen location in Norway and download the data.

Finally, two recommendations are given for further work. Firstly, the spatial mapping component currently is based only on data for individual years and thus the average background concentration given in the maps are only valid for these years. It is recommended to extend the spatial component to several years. This will have two distinct advantages. For one, the maps of the several years can be averages and thus a more representative picture of the “typical” background concentrations can be obtained, just as it was done for the temporal component by averaging station data for the last 5-10 years. Furthermore, several years of data could be used to determine possible trends in the spatial patterns and the overall values, at least within the limits of the uncertainty associated with the estimates of background concentrations.

Secondly, it is recommended to carry out an uncertainty analysis of the data. Both the spatial and the temporal component of the estimation methodology are associated with significant uncertainties from a wide variety of sources such as the input data, the geostatistical interpolation techniques and simplifying assumptions on station representativity. Quantifying these uncertainties is critical for understanding the limitations of the dataset and for being able to make best use of the dataset. Such a task can be accomplished by either performing cross-validation of the existing data or using an independent reference dataset. The result will be uncertainty estimates for both the spatial and temporal component of the methodology and will allow to display reasonable error bars when visualizing the data. This will give the user a much better idea about the usability of the dataset for various purposes and as such enhance its overall value.

Acknowledgements

We are grateful to Etienne Terrenoire, Bertrand Bessagnet, and Laurence Rouil for providing the high-resolution CHIMERE model output.

References

- Bessagnet, B., Hodzic, A., Vautard, R., Beekmann, M., Cheinet, S., Honoré, C., Liousse, C., and Rouil, L. (2004). Aerosol modeling with CHIMERE - preliminary evaluation at the continental scale. *Atmospheric Environment*, 38(18):2803–2817.
- Boersma, K. F., Eskes, H. F., and Brinksma, E. J. (2004). Error analysis for tropospheric NO₂ retrieval from space. *Journal of Geophysical Research*, 109(D4).
- Boersma, K. F., Eskes, H. J., Dirksen, R. J., van der A, R. J., Veefkind, J. P., Stammes, P., Huijnen, V., Kleipool, Q. L., Sneep, M., Claas, J., Leitão, J., Richter, A., Zhou, Y., and Brunner, D. (2011). An improved tropospheric NO₂ column retrieval algorithm for the Ozone Monitoring Instrument. *Atmospheric Measurement Techniques*, 4:1905–1928.
- Boersma, K. F., Eskes, H. J., Veefkind, J. P., Brinksma, E. J., van der A, R. J., Sneep, M., van den Oord, G. H. J., Levelt, P. F., Stammes, P., Gleason, J. F., and Bucsela, E. J. (2007). Near-real time retrieval of tropospheric NO₂ from OMI. *Atmospheric Chemistry and Physics*, 7:2103–2118.
- Bovensmann, H., Burrows, J. P., Buchwitz, M., Frerick, J., Noël, S., Rozanov, V. V., Chance, K. V., and Goede, a. P. H. (1999). SCIAMACHY: Mission Objectives and Measurement Modes. *Journal of the Atmospheric Sciences*, 56(2):127–150.
- Bucsela, E., Celarier, E., Wenig, M., Gleason, J., Veefkind, J., Boersma, K., and Brinksma, E. (2006). Algorithm for NO₂ vertical column retrieval from the ozone monitoring instrument. *IEEE Transactions on Geoscience and Remote Sensing*, 44(5):1245–1258.
- Bucsela, E. J. (2012). A new algorithm for retrieval of stratospheric and tropospheric NO₂ from nadir satellite instruments. *in preparation*.
- Burrows, J. P., Weber, M., Buchwitz, M., Rozanov, V., Ladstätter-Weiß enmayer, A., Richter, A., DeBeek, R., Hoogen, R., Bramstedt, K., Eichmann, K.-U., Eisinger, M., and Perner, D. (1999). The Global Ozone Monitoring Experiment (GOME): Mission Concept and First Scientific Results. *Journal of the Atmospheric Sciences*, 56(2):151–175.
- Chance, K. (2002). OMI Algorithm Theoretical Basis Document - Volume IV: OMI Trace Gas Algorithms. Technical Report ATBD-OMI-04, Smithsonian Astrophysical Observatory, Cambridge, MA, United States.
- Cressie, N. A. C. (1993). *Statistics for spatial data*. Wiley-Interscience, New York.
- Denby, B., Gola, G., de Leeuw, F., de Smet, P., and Horálek, J. (2011). Calculation of pseudo PM_{2.5} annual mean concentrations in Europe based on annual mean PM₁₀ concentrations and other supplementary data. Technical Report ETC/ACC 2010/9, European Topic Centre on Air and Climate Change, Bilthoven, Netherlands.
- Dentener, F., van Weele, M., Krol, M., Houweling, S., and van Velthoven, P. (2003). Trends and inter-annual variability of methane emissions derived from 1979-1993 global CTM simulations. *Atmospheric Chemistry and Physics*, 3:73–88.
- Fagerli, H., Gauss, M., Benedictow, A., Griesfeller, J., Jonson, J. E., Nyiri, A., Schulz, M., Simpson, D., Steensen, B. M., Tsyro, S., Valdebenito, A., Wind, P., Aas, W., Hjellbrekke, A.-G., Mareckova, K., Wankmueller, R., Iversen, T., Kirkevåg, A.,

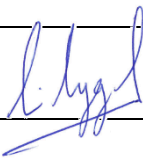
- Seland, O., and Vieno, M. (2011). Transboundary Acidification, Eutrophication and Ground Level Ozone in Europe in 2009 - EMEP Status Report 2011. Technical Report 1/2011, Meteorological Synthesizing Centre - West (MSC-W), Oslo, Norway.
- Goovaerts, P. (1997). *Geostatistics for natural resources evaluation*. Oxford University Press, New York.
- Gottwald, M., Bovensmann, H., Lichtenberg, G., Noel, S., von Bargaen, A., Slijkhuis, S., Pitters, A., Hoogeveen, R., von Savigny, C., Buchwitz, M., Kokhanovsky, A., Richter, A., Rozanov, A., Holzer-Popp, T., Bramstedt, K., Lambert, J.-C., Skupin, J., Wittrock, F., Schrijver, H., and Burrows, J. (2006). *SCIAMACHY - Monitoring the Changing Earth's Atmosphere*. DLR, Institute fuer Methodik der Fernerkundung (IMF).
- Horálek, J., Denby, B., Smet, P. D., Leeuw, F. D., Kurfürst, P., Swart, R., and van Noije, T. (2007). Spatial mapping of air quality for European scale assessment. Technical Report ETC/ACC 2006/6, European Topic Centre on Air and Climate Change, Bilthoven, Netherlands.
- Horálek, J., Smet, P. D., Leeuw, F. D., Conková, M., Denby, B., and Kurfürst, P. (2010). Methodological improvements on interpolating European air quality maps. Technical Report ETC/ACC 2009/16, European Topic Centre on Air and Climate Change, Bilthoven, Netherlands.
- Isaaks, E. H. and Srivastava, R. M. (1989). *Applied geostatistics*. Oxford University Press, New York.
- Levelt, P., van den Oord, G., Dobber, M., Malkki, A., Stammes, P., Lundell, J., and Saari, H. (2006). The Ozone Monitoring Instrument. *IEEE Transactions on Geoscience and Remote Sensing*, 44(5):1093–1101.
- Munro, R., Eisinger, M., Anderson, C., Callies, J., Corpaccioli, E., Lang, R., Lefebvre, A., Livschitz, Y., and Albiñana Perez, A. (2006). GOME-2 on MetOp. In *Proceedings of the 2006 EUMETSAT Meteorological Satellite Conference*, Helsinki, Finland.
- OMI Team (2012). Ozone Monitoring Instrument (OMI) Data User's Guide. Technical Report OMI-DUG-5.0.
- Richter, A. and Burrows, J. P. (2002). Tropospheric NO₂ from GOME measurements. *Advances in Space Research*, 29(11):1673–1683.
- Schmidt, H., Derognat, C., Vautard, R., and Beekmann, M. (2001). A comparison of simulated and observed ozone mixing ratios for the summer of 1998 in Western Europe. *Atmospheric Environment*, 35:6277–6297.
- Schneider, P., Tø nnesen, D., and Denby, B. (2011). Update of Background Concentrations over Norway. Technical Report OR 68/2011, NILU - Norwegian Institute of Air Research, Kjeller, Norway.
- Simpson, D., Fagerli, H., Jonson, J., Tsyro, S., and Wind, P. (2003). Transboundary Acidification, Eutrophication and Ground Level Ozone in Europe - Part I - Unified EMEP Model Description. Technical Report 1/2003, Norwegian Meteorological Institute, Oslo, Norway.
- Vautard, R. (2003). Paris emission inventory diagnostics from ESQUIF airborne measurements and a chemistry transport model. *Journal of Geophysical Research*, 108(D17):1–21.

- Vautard, R., Beekmann, M., Roux, J., and Gombert, D. (2001). Validation of a hybrid forecasting system for the ozone concentrations over the Paris area. *Atmospheric Environment*, 35(14):2449–2461.
- Wackernagel, H. (2003). *Multivariate geostatistics: an introduction with applications*. Springer, Berlin, Heidelberg, New York.



**Norwegian Institute
for Air Research**

NILU – Norwegian Institute for Air Research
P.O. Box 100, N-2027 Kjeller, Norway
*Associated with CIENS and the
Environmental Research Alliance of Norway*
ISO certified according to NS-EN ISO 9001/ISO 14001

REPORT SERIES SCIENTIFIC REPORT	REPORT NO. OR 1/2013	ISBN: 978-82-425-2548-2 (print) 978-82-425-2549-9 (electronic) ISSN: 0807-7207	
DATE 08.03.2013	SIGN. 	NO. OF PAGES 59	PRICE NOK 150.-
TITLE Evaluation of new data sources for improving the estimation of background concentrations in Norway		PROJECT LEADER Philipp Schneider	
		NILU PROJECT NO. O-112091	
AUTHOR(S) Philipp Schneider and Andrzej Obracaj		CLASSIFICATION * A	
		CONTRACT REF.	
QUALITY CONTROLLER: Dag Tønnesen			
REPORT PREPARED FOR Klima- og forurensningsdirektoratet Postboks 8100 Dep 0032 OSLO			
ABSTRACT <p>A previous report (OR 68/2011) described a geostatistical methodology developed for creating a consistent dataset of background concentrations of NO₂, O₃, PM₁₀, and PM_{2.5} in Norway, that are representative of a typical year. The resulting dataset has a resolution of 0.1 degrees by 0.1 degrees and is available at hourly temporal resolution. Based on this existing methodology, this study reports on the evaluation of new data sources as a means of improving such estimates of background concentrations. The potential of satellite-derived NO₂ data is evaluated for guiding the geostatistics-based spatial interpolation procedure of NO₂ station data in Norway. Furthermore, the output from a high-resolution atmospheric model was tested with respect to its capability of improving the spatial and temporal characterization of background concentrations. Finally, an online web mapping system was developed to make the project results easily accessible and to provide basic data analysis and visualization routines for the public.</p>			
NORWEGIAN TITLE Evaluering av nye datakilder for å forbedre estimering av bakgrunnskonsentrasjoner i Norge			
KEYWORDS Air Quality	Environmental Monitoring		
ABSTRACT (in Norwegian)			

* Classification A *Unclassified (can be ordered from NILU)*
 B *Restricted distribution*
 C *Classified (not to be distributed)*

REFERENCE: O-112091
DATE: FEBRUARY 2013
ISBN: 978-82-425-2548-2 (print)
978-82-425-2549-9 (electronic)

NILU is an independent, nonprofit institution established in 1969. Through its research NILU increases the understanding of climate change, of the composition of the atmosphere, of air quality and of hazardous substances. Based on its research, NILU markets integrated services and products within analyzing, monitoring and consulting. NILU is concerned with increasing public awareness about climate change and environmental pollution.